

HASP Student Payload Application for 2024

Payload Title: Ozone Sensor Payload (1)

Institution: University of North Florida (UNF) and University of North Dakota (UND)

Payload Class: SMALL Submit Date: 10/030/2023

Project Abstract:

Ozone in the stratosphere protects us from harmful ultraviolet rays from the Sun. However, ozone in the troposphere, which is closer to the Earth's surface, is hazardous to human health. Based on the success and experience of previous HASP flights, the UNF-UND team proposes the HASP 2024 fight for the fabrication of ozone sensor payload to measure ozone profile in the stratosphere and troposphere. Three different types of nanocrystalline and nanocomposite materials will be used in fabrication of thin film gas sensors arrays. Gas sensors will be mounted on the three sides of the rectangular payload body. Each sensor box will have 8 ozone gas sensors array. Ozone gas sensors will be fabricated and calibrated by the students' team at UNF. The UV light photodiode sensor will be mounted just below the ozone gas sensors box to measure the amount of photovoltage generated by UV sunlight, which will support the science concept of generation of ozone gas in the presence of UV sunlight. The weight of payload with HASP mounting plate will be about 2.75 kg, maximum power drawn will be about 11.1 W and 238 bytes downlink bandwidth. The team consists of six returning and four new students working on the research project. The University of North Florida Space Science & Engineering students' club will participate in the project.

Team Name	<u>.</u>	Team or Project Website: www.ospreyspace-se.org		
Osprey (Ozone Sensor Payload)		J	1 7 1 23328	
Student Team Leader Information:		Faculty Advisor Contact Information:		
Name:	Lovely Ramos (Leader)	Dr. Nirmalkumar G. Patel Dr. Ronald Fevig		
Department:	Electrical Engineering	Physics	Space Studies	
Mailing Address:	University of North Florida Building #50 1 UNF Drive	University of North Florida Building #50 1 UNF Drive	University of North Dakota Clifford Hall, Room 512 4149 Uni. Ave Stop 9008	
City, State,	Jacksonville, FL 32224	Jacksonville, FL 32224	Grand Forks, ND 58202	
Email:	N01486151@unf.edu	npatel@unf.edu	rfevig@space.edu	
Telephone	904-620-2729	904-200-2855	701-777-2480	
Mobile	661-370-5383	904-200-2855	520-820-3440	

HASP2024 Proposal

Ozone Sensors Payload (1)

Submitted by

University of North Florida (UNF) and University of North Dakota (UND)

UNF Students Team:

Lovely Ramos (Leader), Calla Taylor (Deputy Leader)
Dustin Leonard, Colin Ott, Cory Pare, Julian Rowe,
Aryan Patel, Larry Ratcliff, Diya Patel, Elie Ortiz, and Patrick Buckley

Faculty Advisors:

Dr. Nirmalkumar G. Patel (UNF) Dr. Ronald A. Fevig (UND)





Table of Contents				
Section	Content	Page		
	Flight Hazard Certificate Checklist	4		
1	Payload Description	5		
1.1	Payload Scientific / Technical Background	5		
1.1.1	Mission Statement	8		
1.1.2	Mission Background and Justification	8		
1.1.3	Mission Objectives	12		
1.2	Payload Systems and Principle of Operation	15		
1.3	Major System Components	19		
1.4	Mechanical and Structural Design	19		
1.5	Electrical Design	22		
1.6	Thermal Control Plan	23		
2	Team Structure and Management	26		
2.1	Team Organization and Roles	26		
2.2	Timeline and Milestones	29		
2.3	Anticipated Participation in Integration and Launch Operation	30		
3	Payload Interface Specifications	32		
3.1	Weight Budget	32		
3.2	Power Budget	33		
3.3	Downlink Serial Data	37		
3.4	Uplink Serial Commanding	38		
3.5	Analog Downlink	39		
3.6	Discrete Commanding	39		
3.7	Payload Location and Orientation Request	39		
3.8	Special Request	40		
4	Preliminary Drawings and Diagrams	41		
5	References	41		
	Appendix-A (1) Detailed Mechanical Drawings	42		
	Appendix-A (2) Detailed Electronic Circuit Diagrams	59		
	Appendix B: NASA Hazard Tables	67		

Flight Hazard Certification Checklist

NASA has identified several classes of materials that are hazardous to personnel and flight systems. This checklist identifies the documented risks. Applying flight groups is required to determine if the payload includes any of the hazards listed below. Simply place (x) in the appropriate field for each hazard classification. **Note:** Certain classifications are explicitly banned from HASP (grey-filled items in table below) and the remaining hazards will require additional paperwork and certifications. If you intend to include one of the hazards, you must include the detailed documentation in section 3.8 of the application as required by the HASP Call for Payloads. This certification must be signed by both the team faculty advisor and student team lead and included in the application immediately following the cover sheet form.

Hazardous Materials List					
Classification	Included on Payload	Not Included on Payload			
RF transmitters		X			
High Voltage		X			
Lasers (Class 1, 2, and 3R only) Fully Enclosed		X			
Intentionally Dropped Components		X			
Liquid Chemicals		X			
Cryogenic Materials		X			
Radioactive Material		X			
Pressure Vessels		X			
Pyrotechnics		X			
Magnets less than 1 Gauss		X			
UV Light		X			
Biological Samples		X			
Non-Rechargeable Batteries		X			
Rechargeable Batteries		X			
High intensity light source		X			

Student Team Leader Signature:	<i>(</i>	Loudy		Danio	_	
_	0	(Lovely	/ Ran	nos)	5	

Faculty Advisor Signature: Wirmal Halel

(Dr. Nirmalkumar G. Patel) | 0/3 0 | 2.23

1. Payload Description

1.1 Payload Scientific / Technical Background

Ozone in the stratosphere protects us from harmful ultraviolet rays from the Sun. However, ozone in the troposphere, which is closer to the Earth's surface, is hazardous to human health. We recorded 20,000 breaths per day. The air that we breathe has a significant impact on health.

Ozone in the Stratosphere

Generation of Ozone in the Stratosphere: Ozone in the stratosphere is good. Oxygen gas (O_2) was present in the atmosphere. High-energy or shorter-wavelength UV light (hv) collides with the oxygen molecule (O_2) , causing it to split into two oxygen atoms. These atoms are unstable, and they prefer being "bound" to something else. The free oxygen atoms then smash into other oxygen molecules, forming ozone (O_3) .

$$O_2 + hv \rightarrow O_1 + O_1$$

 $O_{1 \text{ (atom)}} + O_{2 \text{ (Oxygen gas)}} \rightarrow O_{3 \text{ (Ozone)}}$

The overall reaction between oxygen and ozone formation is as follows:

$$3 O_2 \rightarrow 2 O_3$$

Ozone is destroyed in the process that protects us from UV-B and UV-C rays emitted by the sun. When ozone (O_3) absorbs UV light (hv), it splits into one free oxygen atom (O_1) and one molecule of oxygen gas (O_2) . Thus, absorption of UV-B and UV-C leads to the destruction of ozone

$$O_{3 \text{ (Ozone)}} + hv \rightarrow O_{1 \text{ (atom)}} + O_{2 \text{ (Oxygen gas)}}$$

Ozone is valuable because it absorbs harmful UV radiation during the destruction process. Dynamic equilibrium is established in these reactions. The ozone concentration varies according to the amount of radiation received from the sun.

Ozone in the Troposphere

Generation of Ozone in the Troposphere: Ozone in the troposphere is poor. Ozone contributes to smog and greenhouse gases created by human activities. Ozone close to the ground surface does not exist at sufficiently high concentrations to shield us from UV light.

Formation of tropospheric ozone

- are VOC (RH), OH (hydroxyl radical), NOx, and M (inert body, N_2 , or O_2); O_3 can be dissociated by UV and forms two OH \rightarrow chain processes.
- VOC and NO_x concentrations control ozone concentrations in a complicated way
- O₃ formation is probably NOx-limited rather than VOC formation.

The formation of tropospheric ozone is as follows:

- VOCs: volatile organic compounds, mostly emitted by motor vehicles, vegetation, industrial and commercial, dry cleaners, and paints.
- NOx: nitrogen oxides, motor vehicles, power plants, industrial facilities, biomass burning, lightning. Sunlight, higher temperature, and low wind speed

The tropospheric ozone affects meteorology.

- Higher O₃ concentrations were found in the summer under dry high-pressure conditions.
- during inversions (warm air above cooler air), pollutants are often trapped, resulting in high ozone concentrations and nocturnal ozone maxima at nighttime.

Tropospheric or ground-level ozone is the major ingredient in smog and poses health risks.

- Ozone attacks cells and breaks down the tissue.
- decreased the ability to breathe and cough and increased susceptibility to respiratory diseases, such as pneumonia and bronchitis. Increased sensitivity to allergens.
- Long-term exposure to radiation may result in permanent lung damage.
- According to the EPA, approximately 15,000 Americans die annually from exposure to airborne pollutants, and exposure to ozone causes hundreds of thousands of acute asthmas.
- Ozone is a plant toxin enforced by the presence of SO₂ and NO_x.
- Ozone also damages materials, such as nylon, rubber, and certain fabrics.
- Economic impacts and damage to agricultural crops, forests, and wilderness areas.
- Lowering ozone levels by 25% may increase the US crop yield by \$0.5 to 1.0 billion per year.
- The natural tropospheric ozone concentration was 10 ppb. However, higher levels are detrimental to health.

In establishing the 8-hour standard, EPA is setting the standard at 0.08 parts per million (ppm) and defines the new standard as a "concentration-based" form, specifically the 3-year average of the annual fourth-highest daily maximum 8-hour average ozone concentrations.

Ozone Hole

The criticality of the ozone layer can be understood from the fact that only ten or less of every million molecules of air are ozone. Many of these ozone molecules reside in a layer between 10 km and 40 km above the Earth's surface, known as the stratosphere. Each spring in the stratosphere over Antarctica (the spring in the southern hemisphere is from September to November). Chemical processes can rapidly destroy atmospheric ozone. As winter arrives, a vortex of wind develops around the pole and isolates the polar stratosphere. When the temperature drops below -78°C, thin clouds form from the ice, nitric acid, and sulfuric acid mixtures. Chemical reactions on the surfaces of ice crystals in clouds release active forms of CFCs. Ozone depletion begins, and an ozone "hole" appears. Approximately 50% of the total column amount of ozone in the atmosphere disappears within two—three months. At certain levels, the losses approached 90%. This is known as the Antarctic ozone hole. In spring, the temperature begins to rise, ice evaporates, and the ozone layer starts to recover. Thus, ozone "hole" is a reduction in concentrations of ozone high above the earth in the stratosphere. The

ozone hole was defined geographically as the area where the total ozone amount was less than 220 Dobson Units. The ozone hole has grown steadily and length of existence over the past two and a half decades. The size of the ozone hole in Antarctica was estimated to be 30 million sq. km. Human-caused chlorines, primarily chlorofluorocarbons (CFCs), contribute to thinning of the ozone layer and allow larger quantities of harmful ultraviolet rays to reach the earth.

Nocturnal Ozone

The observed higher concentration of ozone at nighttime due to nocturnal ozone maxima observed in ozone episode areas as bad ozone can be correlated with vertical mixing of the remnant daytime boundary layer. This mixing is forced by an increase in wind speed above the nocturnal surface inversion (fig 1 (a)). Samson [1] proposed that this process not only explains nighttime increases in ozone concentrations at lower altitude and process responsible for the reversed diurnal ozone fluctuations at higher altitude. Investigators [2-3] have shown that higher ozone concentrations occur on the back side of surface high-pressure systems, where the air circulating poleward has an above-average dry-bulb and dew point temperature.

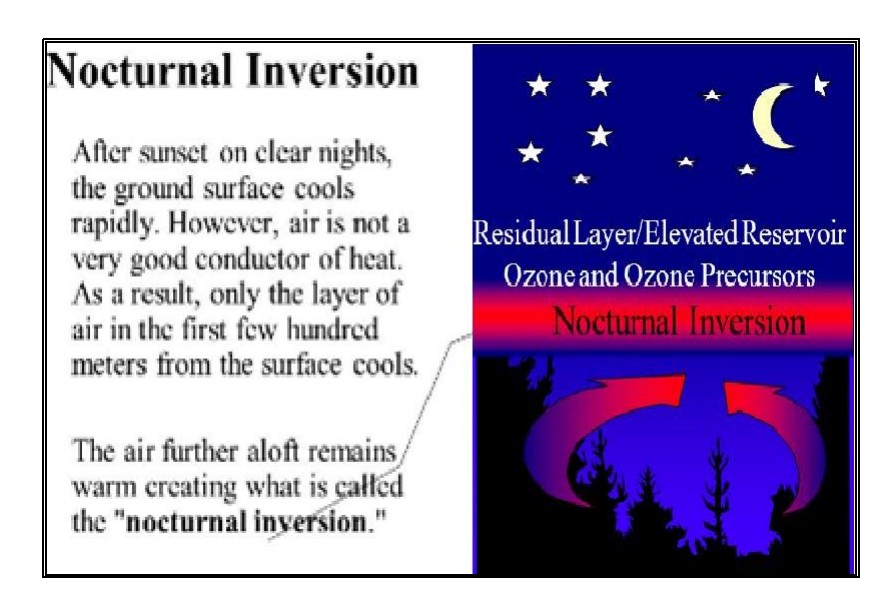


Fig. 1 (a) Formation of Nocturnal Ozone Courtesy: http://slideplayer.com/slide/5314464/

Considering the global issue of bad ozone and ozone depletion and the limitations of ground-based and airborne measuring methods, we have been working on the development of space grade ozone sensors and low weight sensor payloads to measure the ozone profile in the troposphere and stratosphere in real-time mode using the NASA-HASP balloon flight since 2008. The purpose of this work is to develop a thermally stable, highly selective, and sensitive miniature nanocrystalline thin film ozone sensor and payload to substitute conventional methods. These sensors have (i) no

electromagnetic and radio frequency interference, (ii) a larger operational lifetime, and (iii) better accuracy in measuring very low concentrations of ozone (below 1 ppm).

1.1.1 Mission Statement

Nanocrystalline oxide semiconductor thin-film gas sensor array technology (U. S. Patent No. 10,823,690 B2 and 9,606,078 B2) [4, 5] and ITO-QCM (Quartz Crystal Microbalance) sensor platform technologies (U.S. Patent No. 7,930,923 B2) [6] were developed by Dr. Patel at the University of North Florida (UNF) for the detection of ozone, toxic gases, explosive materials, and chemical warfare agents with support from the Edgewood Chemical Biological Center, US Army Laboratory, Aberdeen Proving Ground, and the U.S.. Department of Defense. Nanocrystalline gas sensors have also been used to detect ozone gas in the stratosphere. Nanocrystalline indium tin oxide (ITO) gas sensors were successfully tested and calibrated with ozone gas at the Kennedy Space Center (KSC) and UND between 2008-2009 [7]. The UNF team is improving the performance of ozone sensors by changing their fabrication conditions and modifying their surface structure every year after HASP balloon flight. These sensors were successfully tested on HASP flights. We have made a step-by-step improvement of the sensors by changing the sensing materials, design and fabrication parameters, and hardware and software of the payload every year. UNF ozone sensors were also used by students at Louisiana State University, University of Central Florida, Iowa State University, and Taylor University for their weather balloon projects.

The proposed mission is to fabricate a new, improved ozone gas sensor payload. A new payload has several unique features. ITO gas sensor arrays have higher sensitivity and stability because of their nanocrystalline and nanocomposite thin film structures. Earlier reported work on tungsten oxide sensors for the detection of ozone gas [8] required a high operating temperature of approximately 450°C to detect ozone. The UNF developed nanocrystalline ITO sensor arrays operating at room temperature did not require a heater, which ultimately saved power requirements and space and minimized the possibility of an accidental fire. The UNF developed an alpha phase of silver tungstate thin-film gas sensors with better sensitivity and selectivity for the detection of ozone gas at low pressure, while nanocomposite WO_{3-x} +ITO and Al-doped ZnO +ITO thin-film gas sensors have better selectivity for the detection of ozone in pollutant gases and smog. The UNF-developed gas sensor arrays are very small in size, have low weight, and low power consumption, which meets the payload requirements for space applications.

1.1.2 Mission Background and Justification

Pervious HASP Flight 2023

The proposed study is a continuation of the previous two HASP flights. An overview of the output of the last HASP 2023 flight is presented in Fig.1 (b). A picture of the ozone sensor payload,

payload-HASP in the stratosphere, and flight profile are also shown in fig. 1(b). The responses of the UV photosensors mounted on the three sensor boxes are shown in fig. 1 (c).

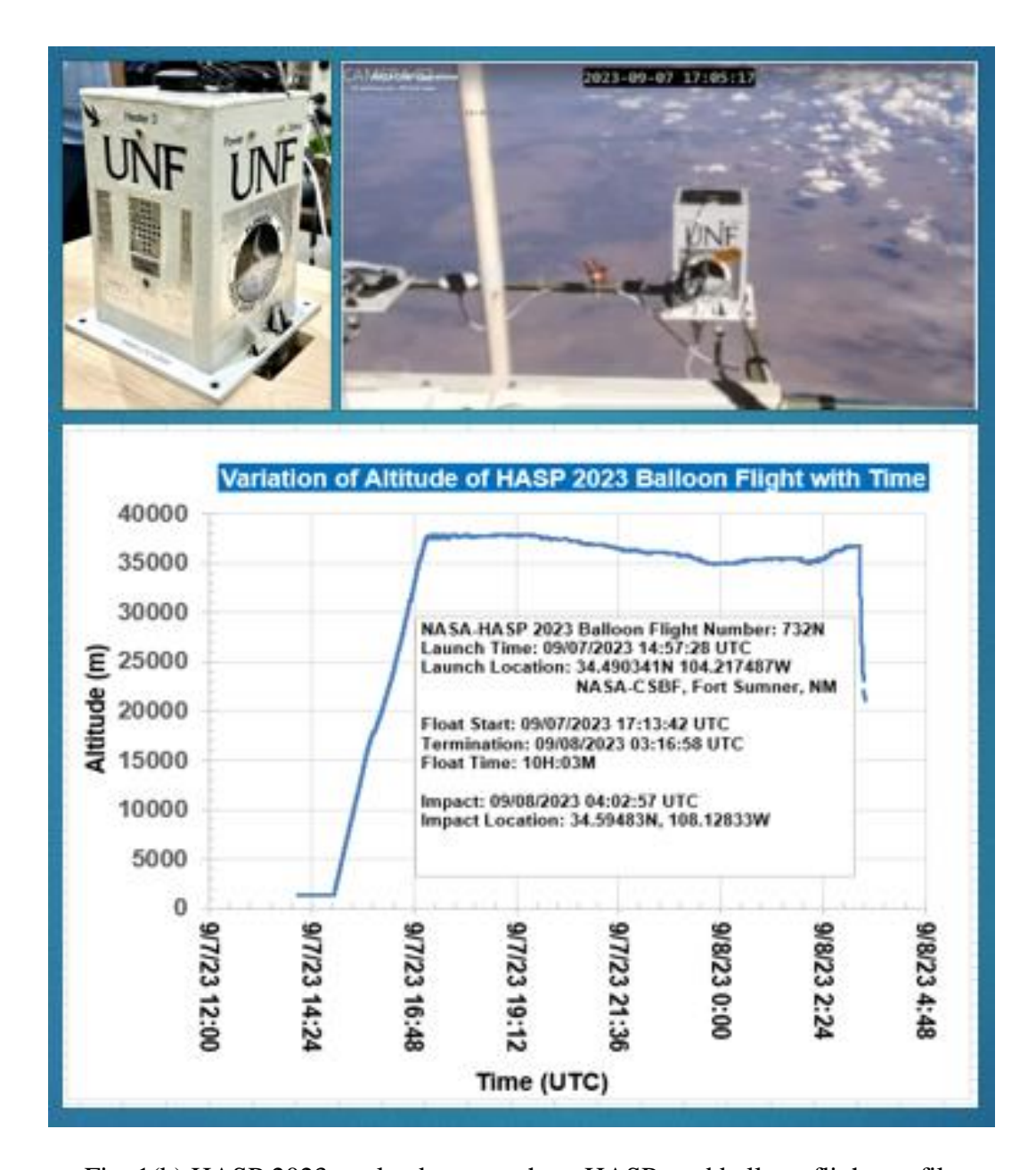


Fig. 1(b) HASP 2023 payload, stratosphere HASP, and balloon flight profile.

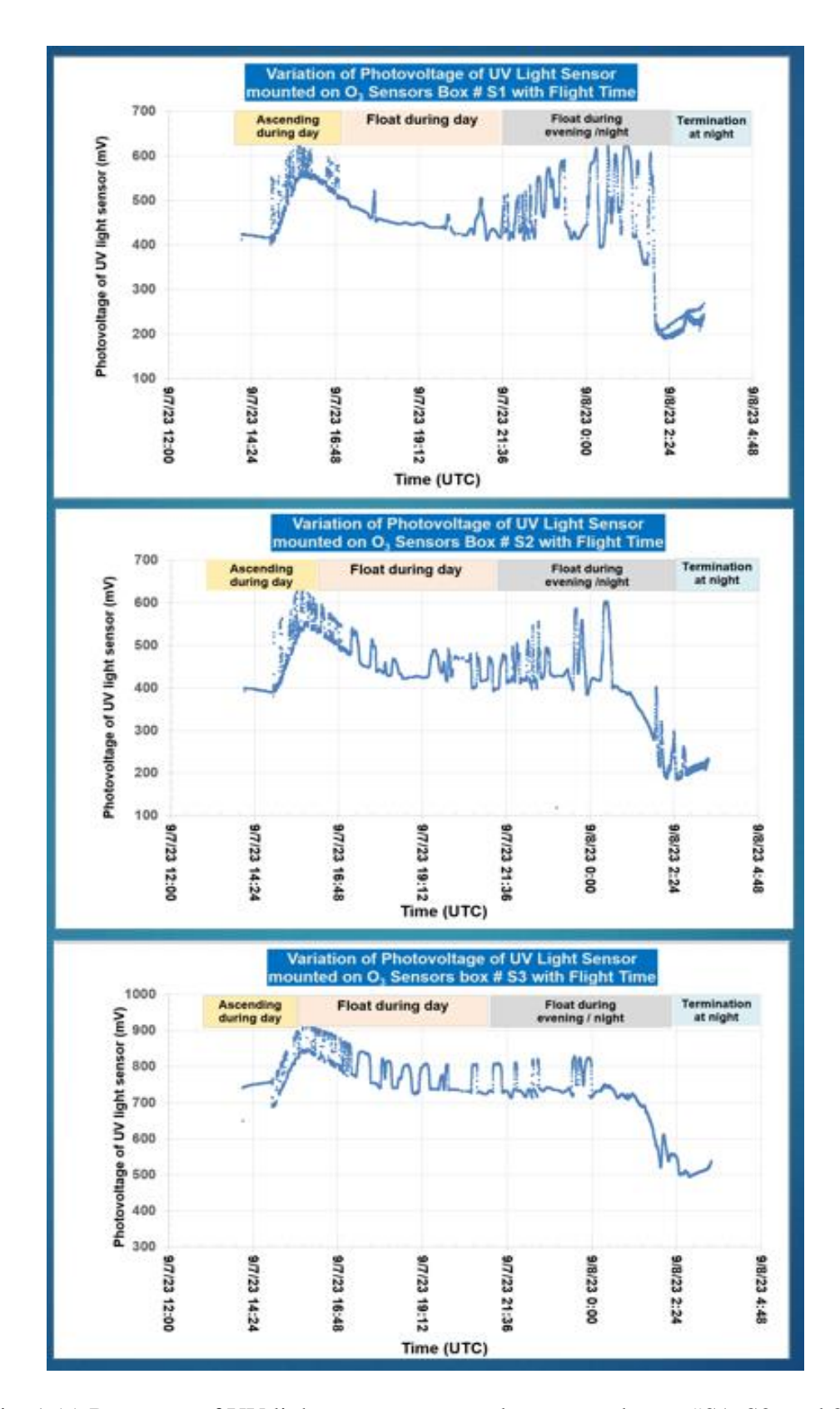


Fig. 1 (c) Response of UV light sensors mounted on sensor boxes #S1, S2, and S3.

The ozone profiles measured by two different types of ozone sensors, S1-2 and S2-7, during the HASP 2023 flight are shown in fig. 1(d) and (e). The ozone concentration varied with altitude each year.

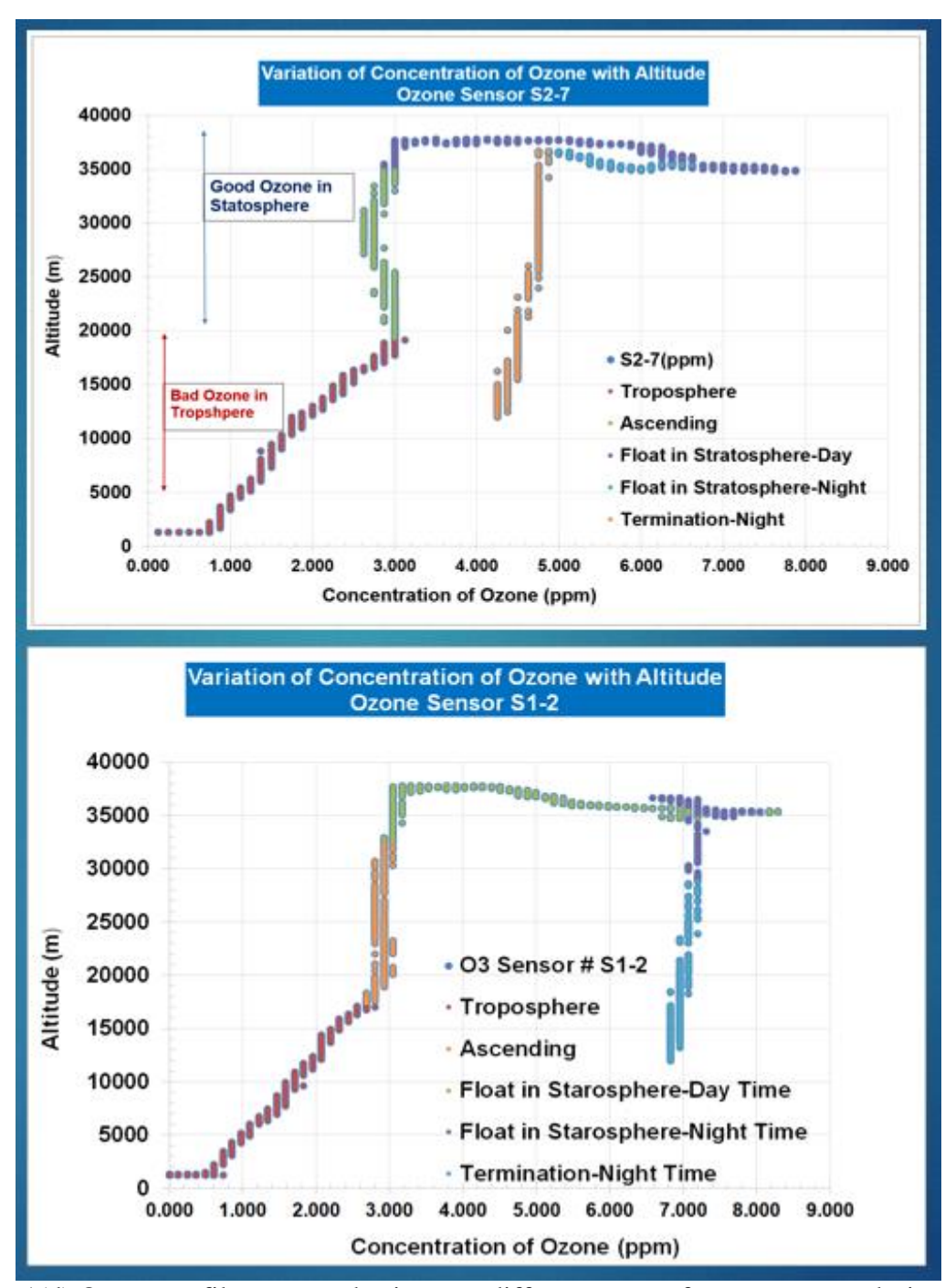


Fig. 1(d) Ozone profile measured using two different types of ozone sensors during the HASP2023.

1.1.3 Mission Objectives

Based on the success and motivation of the HASP balloon flights made during previous flights, the UNF-UND team proposed a HASP 2024 flight with the following objectives for measuring the ozone profile in the stratosphere using the gas sensor payload.

(i) Objectives of nanocrystalline thin film gas sensors boxes

Sensors Box # 1

An improved version of a nanocrystalline ITO thin-film gas sensor array (Box#1) has better thermal stability and selectivity for the detection of ozone gas.

Sensors Box # 2

Improved versions of nanocrystalline WO₃ thin-film gas sensors with better sensitivity for the measurement of ozone gas.

Sensors Box# 3

An updated version of nanocrystalline In₂O₃ thin-film gas sensors will be used to measure the bad ozone in pollutant gases and smog. The new version may include a combination of single-walled carbon nanotube (SWCNTs) -In₂O₃ to enhance selectivity.

UNF students will fabricate ITO thin-film gas sensors using an electron beam deposition method in Dr. Patel's research laboratory. Three sensor boxes (#1, # 2, and # 3) will be mounted on the three sides of the rectangular payload body.

We are interested in adding nano-ozone sensors that are smaller in size to achieve better performance by reducing the number of grain boundaries. We are currently working on the development and fabrication of nanosensors using Electron Beam Lithography (www.raith.com), attached to a Scanning Electron Microscope (FEI, Quanta 200D). We may use nano gas sensors in the 2023 flight if we are fully satisfied with the performance of gas sensors in our laboratory.

All ozone gas sensors were tested and calibrated simultaneously in a low-pressure chamber to minimize the experimental error for the determination of the trend line equations of the plots for converting the electrical resistance values into the concentration of ozone in parts per million (ppm). The pressure and temperature inside the test chamber were maintained as in the stratosphere for good ozone measurements. Ozone sensors will also be tested and calibrated under tropospheric and atmospheric conditions with appropriate pressure and temperature ranges for measurements of bad ozone and nocturnal ozone.

(ii) UV light sensors

We will use all new GaP (FGAP71) UV light photodiodes mounted below the ozone sensor box. The UV-light sensor was maintained at a constant temperature.

This GaP (FGAP71) photodiode had a wavelength range of 150–550 nm and a peak wavelength of 440 nm, as shown in Fig. 1(e).

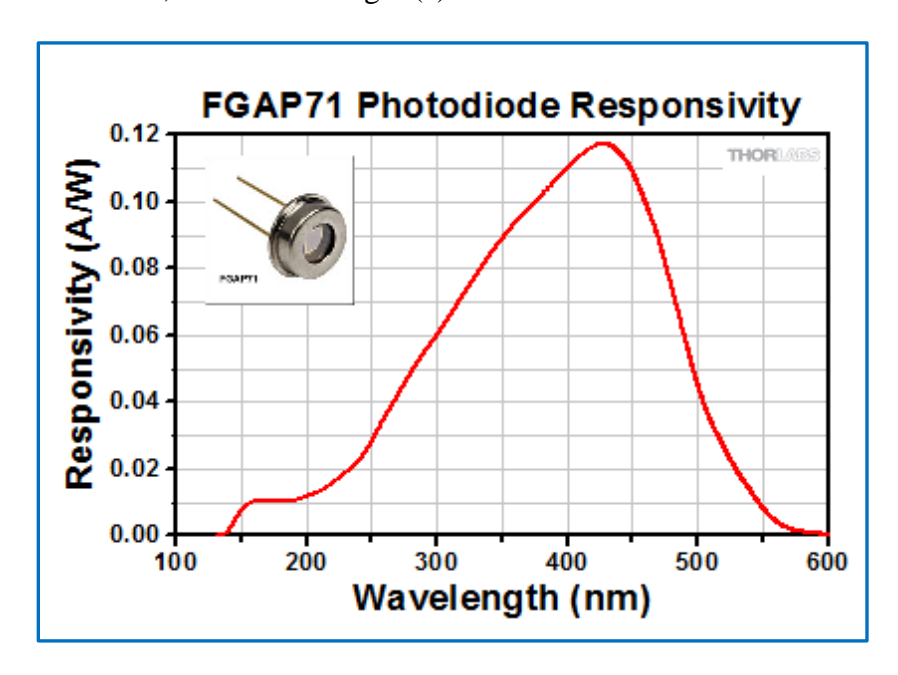


Fig. 1(e) Response of GaP (FGAP71) photodiode (Courtesy: www.thorlab.com) http://www.thorlab.and.com/newgrouppage9.cfm?objectgroup_id=285&pn=FGAP71.

The photodiode was mounted just below the gas sensor box on each side of the payload body. Photodiodes will support the verification of the scientific concept of ozone generation in the presence of UV light. The amount of photovoltage generated and measured by the photodiodes indicates the amount of UV light available to interact with oxygen to convert into ozone gas near ozone gas sensors. Our gas sensor arrays detect and measure the concentration of the ozone gas generated. This **scientific concept** will also help us to understand the effect of any shadow or darkness on the sensor surface, particularly at the time of sunset and decrease in ozone concentration at nighttime.

(iii) New Low-Pressure Sensor

It was observed that the pressure sensor used in the previous flight was operated from atmospheric pressure to 100 mbar and then saturated. We propose to replace it with a new pressure sensor that can measure pressures up to 10 mbar or below.

The new sensors may be purchased from

- (i) http://www.meas-spec.com/product/Pressure/MS5540C.aspx or
- (ii) http://www.omega.com/pptst/PX170.html

We need to adjust the power and space to replace the new pressure sensor; otherwise, we will continue to use the same pressure sensors used in the previous payloads.

(iv) **GPS**:

The current UBLOX GPS worked well during the last several flights and was not blocked at high altitudes. The GPS antenna was installed away from the payload body and worked well. We again used the same GPS. The payload GPS data were cross-verified and compared with HASP GPS data.

(v) Improved and thermally stable payload body.

A single hollow aluminum tube structure was used to create the payload body. The bodywork was almost the same as that during the previous flight. This design reduces the number of screws and nuts, and hence the weight of the payload. This also allows us to easily open and close the payload for access to the hardware. We aimed to reduce the mass of the body. The inner surface of the body has very low outgassing at low pressure and good reflection of Infrared light and heat.

A thermal blanket made of an aluminized heat barrier with an adhesive backed (Part No. 1828 or equivalent) (Make: www.PegasusAutoRacing.com) will be applied to the payload to improve thermal stability. The silver surface of the thermal blanket has high reflection with a wide range of wavelengths of light, and hence is capable of withstanding radiant temperatures more than 1000°C as shown in Fig. 1(f). The payload covered with a thermal blanket and ozone sensors maintained at a constant temperature by the digital temperature controller provides the sensor payload under isothermal conditions for better thermal stability.

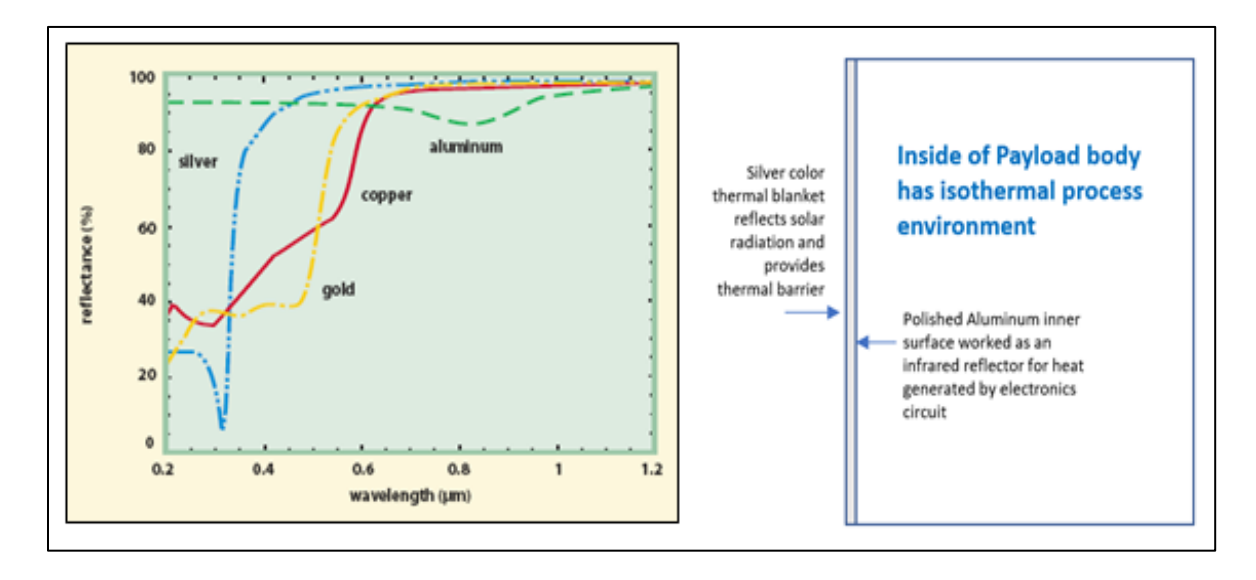


Fig.1 (f) Variation of reflectance with wavelength of light from different color of surfaces Courtesy: http://www.photonics.com/EDU/Handbook.aspx?AID=25501

(vi) Improved version of software

The New JAVA based software allows us to convert all RAW files directly into one EXCEL file. Then, calibration trend line equations were applied to convert the change in

resistance values of sensors into the concentration of ozone gas in ppm. In addition, the new LabVIEW program allows us to quickly monitor the data and view the plots during the thermal vacuum test and flight.

(vii) Use of SEM+EDAX

The surface topography of the sensors before and after the flight was studied using a scanning electron microscope (SEM) (FEI, Quanta 200D), and the chemical composition of the surface of the sensors was analyzed by energy dispersive analysis of X-rays (EDAX) at the UNF under the supervision of Dr. Patel.

(viii) Testing of the payload

Students perform electronic hardware and software testing of the payload at the UNF. They will also perform mechanical tests, including shock and stress analyses, using a simulation program. They also estimated the thermal stability of the PCB and the sensor boxes at low and high temperatures under low and high vacuum in a vacuum chamber. All tests will be performed before the integration of the payload workshop at Palestine, TX. After the flight, the team performs a failure analysis and data analysis and prepares the final science report.

(ix) Deliverable of HASP 2024

Working as a team, submission of monthly science report, participation in monthly videoconference, fabrication of the working payload, testing and integration of payload with HASP at CSBF, Palestine, launching the payload and data collection, data analysis, and submission of the final science report.

1.2 Payload Systems and Principle of Operation

Nanocrystalline thin-film gas sensor arrays will be fabricated on ultrasonically and chemically cleaned glass substrates. The development of a thin film of oxide semiconductor sensor was part of three U.S. Patented sensor platform technologies were invented by Dr. Patel at UNF [6-8]. Fig. 2(a) shows the top view of the eight sensor arrays and the interface printed circuit board. Fig. 2(b) shows a scanning electron micrograph of one ITO thin-film gas sensor with two gold electrodes for the external electrical contacts. Fig.2(c) shows a scanning electron micrograph of the nanocrystalline gains of the ITO thin film, and the sensor boxes are shown in fig. 2(d).

The payload consisted of three sensor boxes with three different types of gas sensors made of different materials.

Box #1: An improved version of the nanocrystalline ITO thin-film gas sensor array (Box#1) has better thermal stability and selectivity for ozone gas detection.

Box #2: Improved version of nanocomposite and nanocrystalline $WO_3 + ITO$ thin-film gas sensors with better sensitivity for the measurement of ozone gas.

Box#3: A new version of nanocrystalline In_2O_3 thin-film gas sensors will be used for the measurement of bad ozone in pollutant gases and smog. The new version may include a combination of single-walled carbon nanotube (SWCNTs) - In_2O_3 to enhance selectivity.

Sensors will work better for the measurement of bad ozone in the troposphere and the atmosphere.

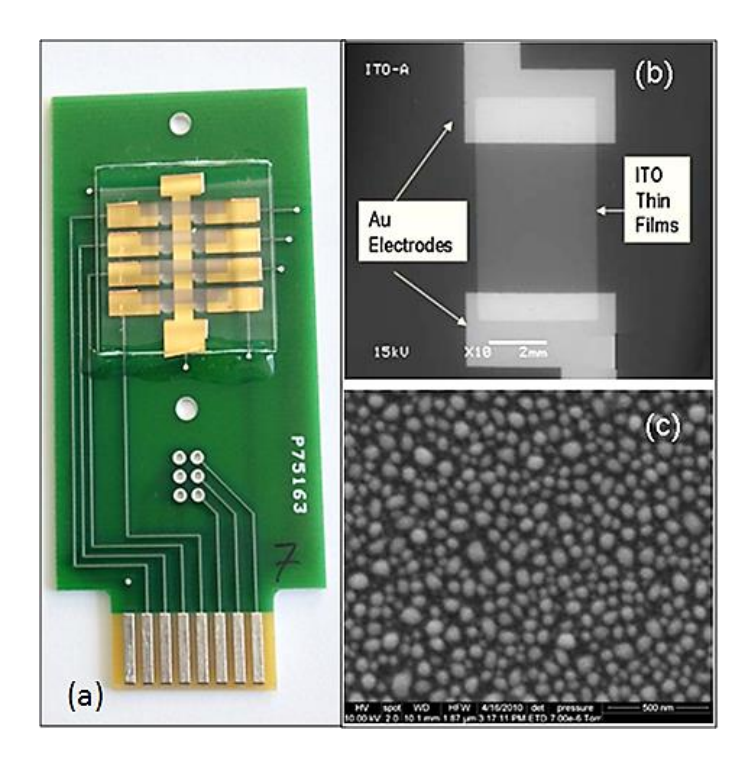


Fig.2 (a) Eight sensor array and interface mini-PCB, scanning electron micrograph of (b) top view of one ITO gas sensor, and (c) nanocrystalline grains of ITO thin film.

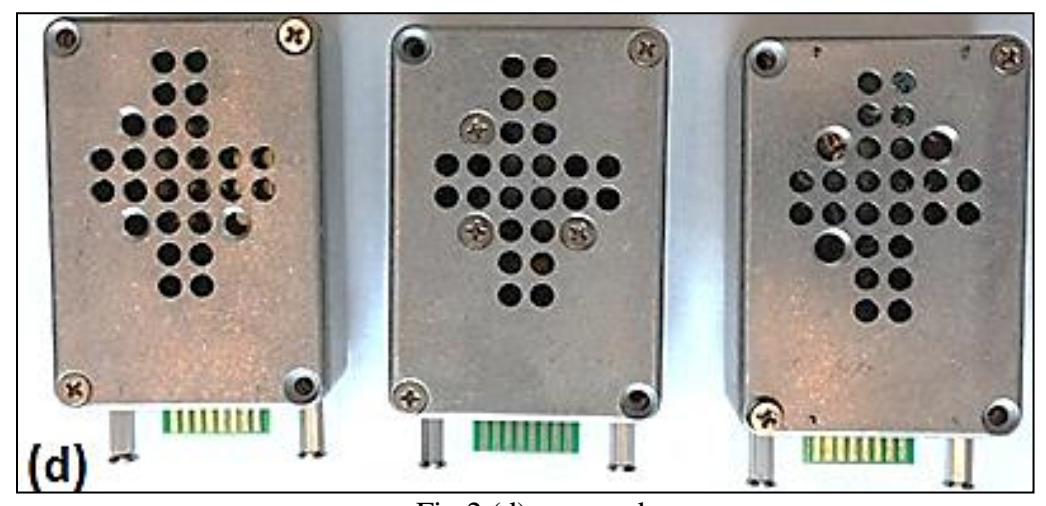


Fig.2 (d) sensors boxes

Each type of sensor array box has different sensor characteristic parameters for gas detection. Three different types of gas sensor array boxes were fabricated at the UNF.

Fig. 3 (a) shows a picture of the housing for the UNF sensors, consisting of an array of eight gas sensors interfaced with a printed circuit board (PCB), flexible Kapton heater (MINCO make HK 5573R30.0 L12BU), a temperature sensor (Analog Device TMP36), an electrical fan (SUNON, MC25060V2-0000-A99, DC 5V, 0.38 W) and a 16 wires flat cable. One end of the flat cable has a female card edge connector to connect to the sensor PCB (Make 3M, MCS16K-ND), while the other end has 16 pin females to connect to the microcontroller PCB.

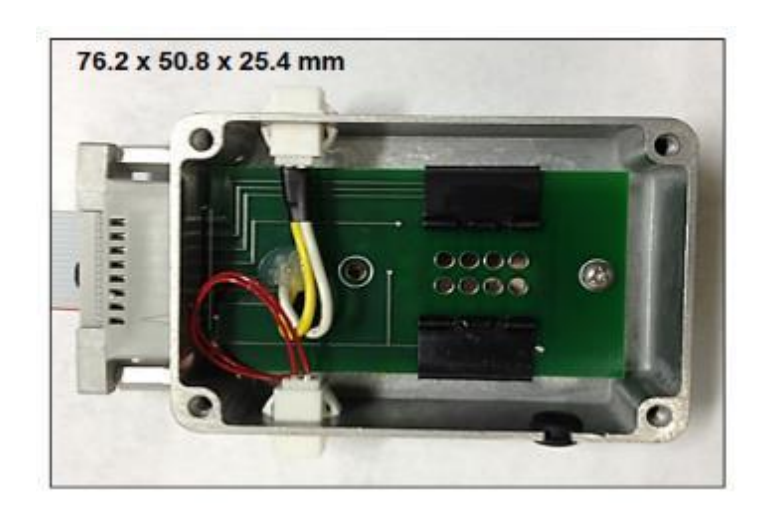


Fig. 3(a) shows a photograph of the payload sensor box. The sensor box consists of eight ozone sensor arrays mounted on a PCB with one heater, a miniature fan, and a temperature sensor.

The sensor array was interfaced with the printed circuit board and its 16-pin female card edge connector and a flat cable. The sensors were tested and calibrated with ozone under low pressure at the UNF. An ozone generator (Ozone Solutions, Model# OMZ-3400) was used as the ozone source, which generated 0–12 ppm ozone gas. A digital ozone detector (Eco Sensors, Inc., Model:A-21ZX) was used to measure the ozone concentration. A Keithley electrometer and multimeter with LabVIEW software were used to simultaneously measure the resistance of all sensors in the test chamber. The parameters of the trendline equations of the calibration plots were used to determine the ozone concentration.

Working Principle of Gas Sensors

Interaction of oxidizing gas on surface of n-type ITO thin film sensor

Upon adsorption of charge-accepting molecules at the vacancy sites, namely, from oxidizing gases such as ozone (O₃), these electrons are effectively depleted from the conduction band of ITO. This leads to an increase in the electrical resistance of the n-type ITO.

For example, ozone gas

Oxygen vacancy (V) + Ozone (O₃) \rightarrow Lattice Oxygen site (O₀) + O₂

Vacancies can be filled by reaction with ozone. Filled vacancies are effective electron traps, and consequently, the resistance of the sensor increases upon reacting with ozone.

Interaction of reducing gas on surface of n-type ITO thin film sensor

Oxygen vacancies on the ITO surfaces are electrically and chemically active. These vacancies function as n-type donors, decreasing the electrical resistivity of ITO. Reducing gases such as CO, H₂, and alcohol vapors results in detectable decreases in the electrical resistance of n-type ITO.

For example: methanol:

CH₃OH (methanol) + O⁻ (chemisorbed ion on surface of ITO)

→ HCOH (Formaldehyde) + H₂O (water) + e⁻ (electron)

Vapors encounter the surface, react with chemisorbed oxygen ions O- or O²-, and re-inject electrons into the conduction band.

In summary, the electrical resistance of ITO increases in the presence of oxidizing gases such as ozone. Upon adsorption of the charge-accepting molecules at the vacancy sites, namely oxidizing gases such as ozone, electrons are effectively depleted from the conduction band, leading to an increase in the electrical resistance of the n-type ITO. Our three types of sensor boxes are n-type semiconductor gas sensors.

Steps for Measurements of Ozone

Fig. 3(b) shows various steps for the detection of ozone by the sensor payload during flight, and the detection of reducing gases will also have similar steps. The team developed a program to evaluate the HASP payload. Quick monitoring of data directly from the LSU website server is possible. This LabVIEW-based program saves time by downloading the files and then applies a software program to put data in EXCEL and then make plots. This will help us easily monitor the data during the thermal vacuum test as well as during flight.

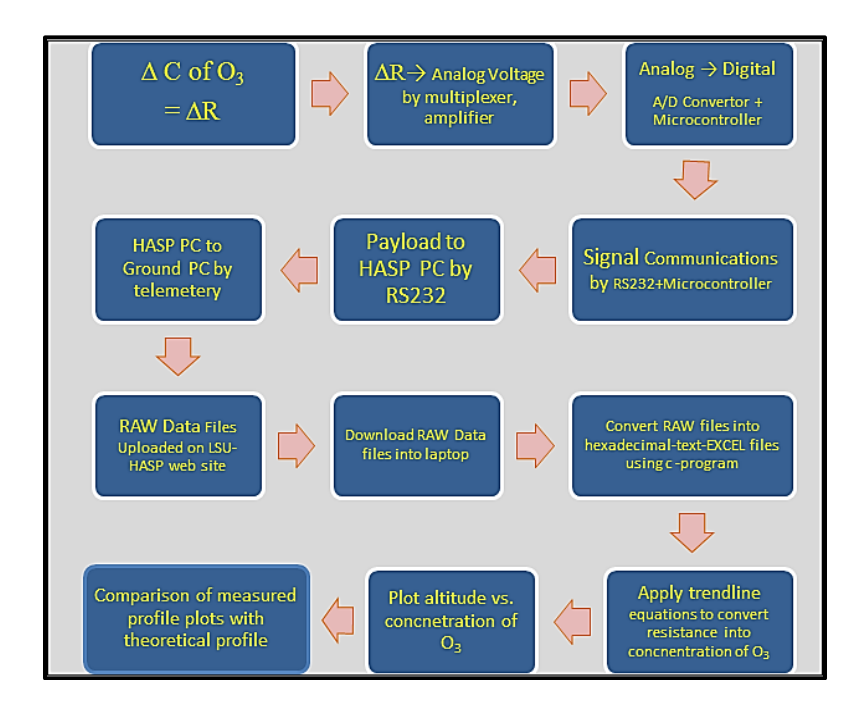


Fig. 3(b) Steps for the detection of ozone by the payloa

1.3 Major System components

The payload consists of three sensor boxes. Each sensor box had eight gas sensors, one flexible heater, one temperature sensor, and one mini-fan. The boxes of the three sensors are mounted on three sides of the cubic payload body. Gas molecules can enter the sensor box through the perforated holes in the payload body. The fan protects the surface of the sensor by blowing dust particles into the atmosphere and ice particles in the troposphere. The temperature of the ozone gas sensor was maintained at approximately $305\pm5^{\circ}$ K using a temperature controller. A flexible heater (MINCO or OMEGA make) and a temperature sensor (Analog Device TMP 36) were mounted on the back side of the gas sensors. All gas sensors, UV light sensors, GPS, pressure sensors, and temperature sensors were interfaced with a microcontroller circuit board.

1.4 Mechanical and Structural Design

The important features of our payload body are easy to open and close, easy access to PCB and sensor boxes, low rate of outgassing under low pressure, better stability with thermal and impact, and reusability. The payload metal parts were procured payload from the supplier www.onlinemetals.com.

The payload continues to feature a rectangular design due to its robustness as well as for its low rate of outgassing under extreme pressure drops. This design is optimal for the team's goal of achieving a reusable payload body. The details of the design, drawing, and fabrication are shown in fig.4 (a) to (u). Cory Pare designed the proposed payload using SolidWorks and AutoCAD. UNF students will fabricate the payload body in the UNF workshop. The outer dimensions of payload body will be about 228.6 mm height, 152.4 mm depth and 152.4 mm width.

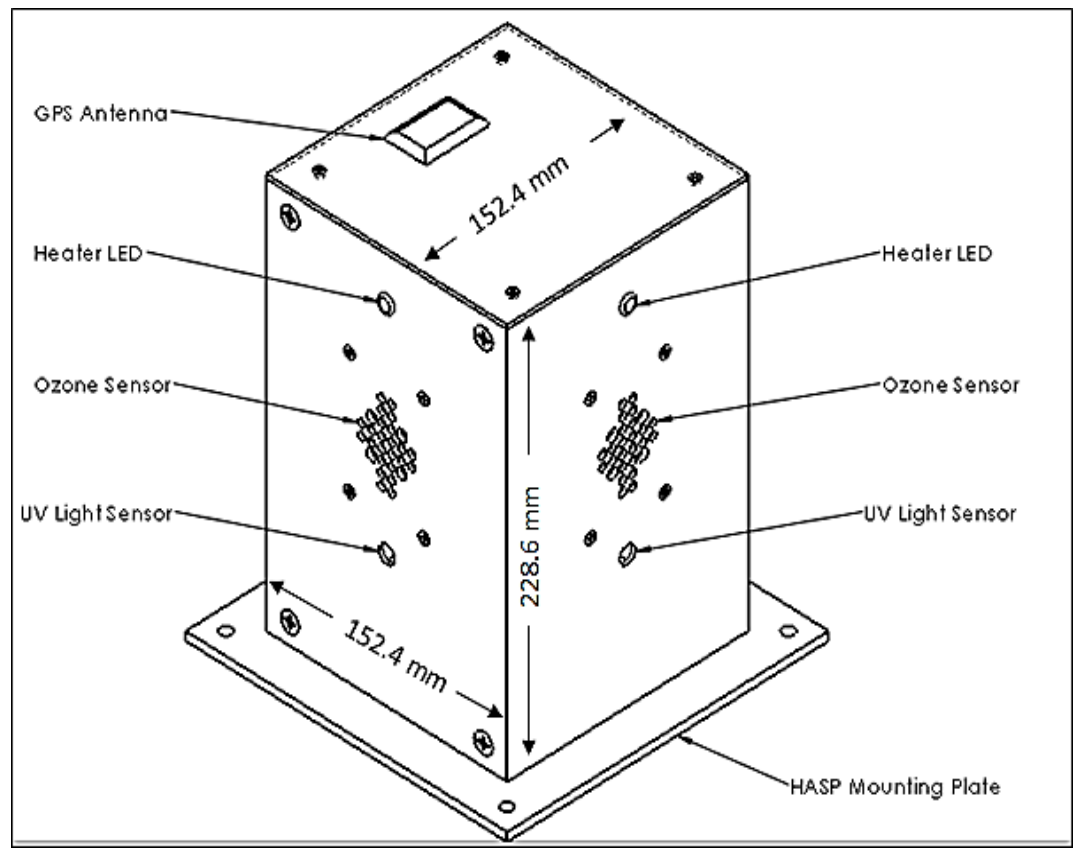
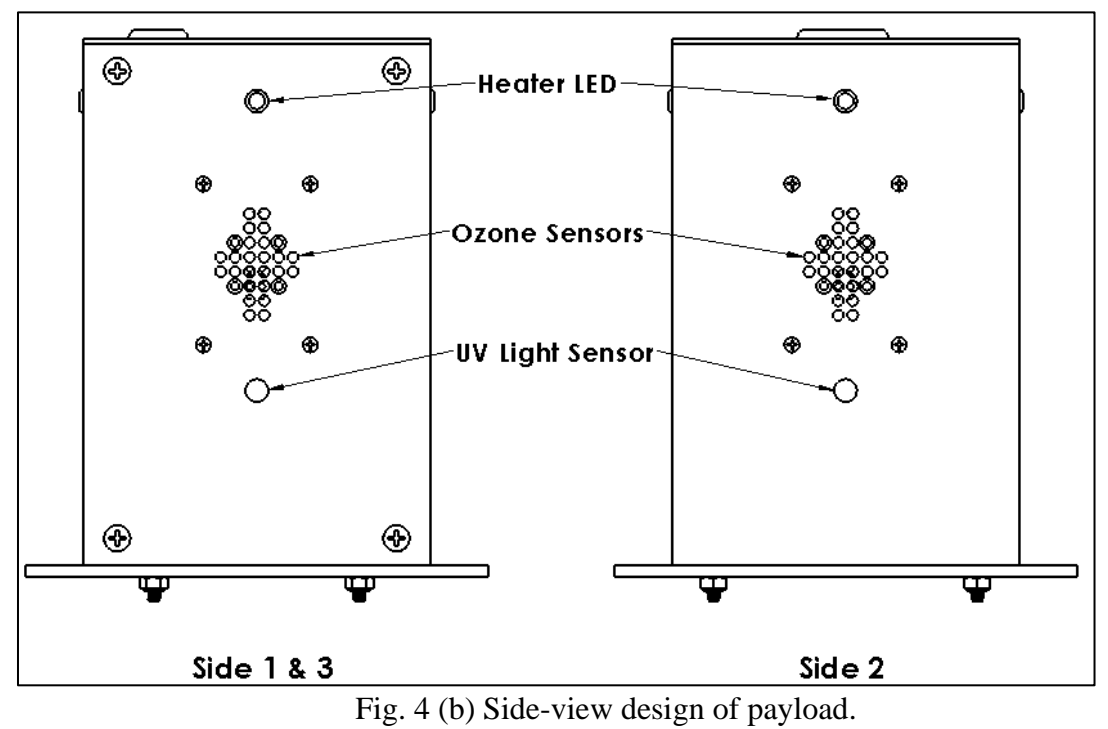


Fig.4 (a) Design of payload body.



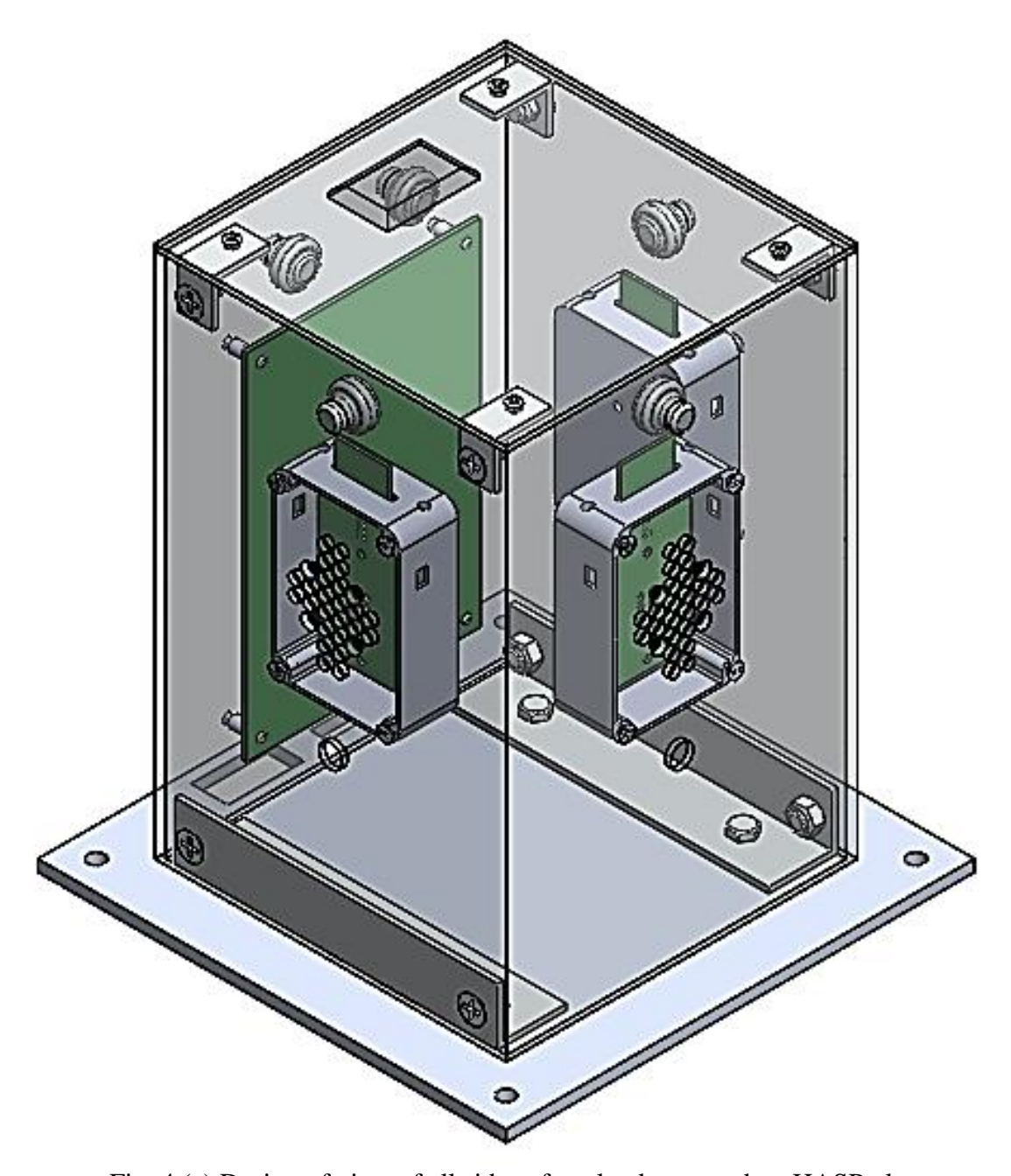


Fig. 4 (c) Design of view of all sides of payload mounted on HASP plate.

The payload was mounted on a HASP mounting plate using aluminum L-brackets, bolts, washers, and nuts. We will ensure that the payload is well secured so that it remains intact and attached to the HASP mounting plate under a 10 g vertical and 5 g horizontal shock. In addition, the payload body is aluminum, so it will certainly survive and operate in the very low-pressure range of 5 to 10 millibars at the float altitude.

The details of the mechanical drawings are shown in fig. 15(a)–15(p).

Please refer to Appendix A (1) on page 42-59.

Payload Mounting Footprint

The selection of a small payload dictates the mounting plate that interfaces with it. This mounting plate design is provided in the HASP Student Payload Interface Manual (Version 02.17.09) and is illustrated in Fig.5. This mounting plate design does not require any modification, except to make four mounting holes, as shown in fig. 5.

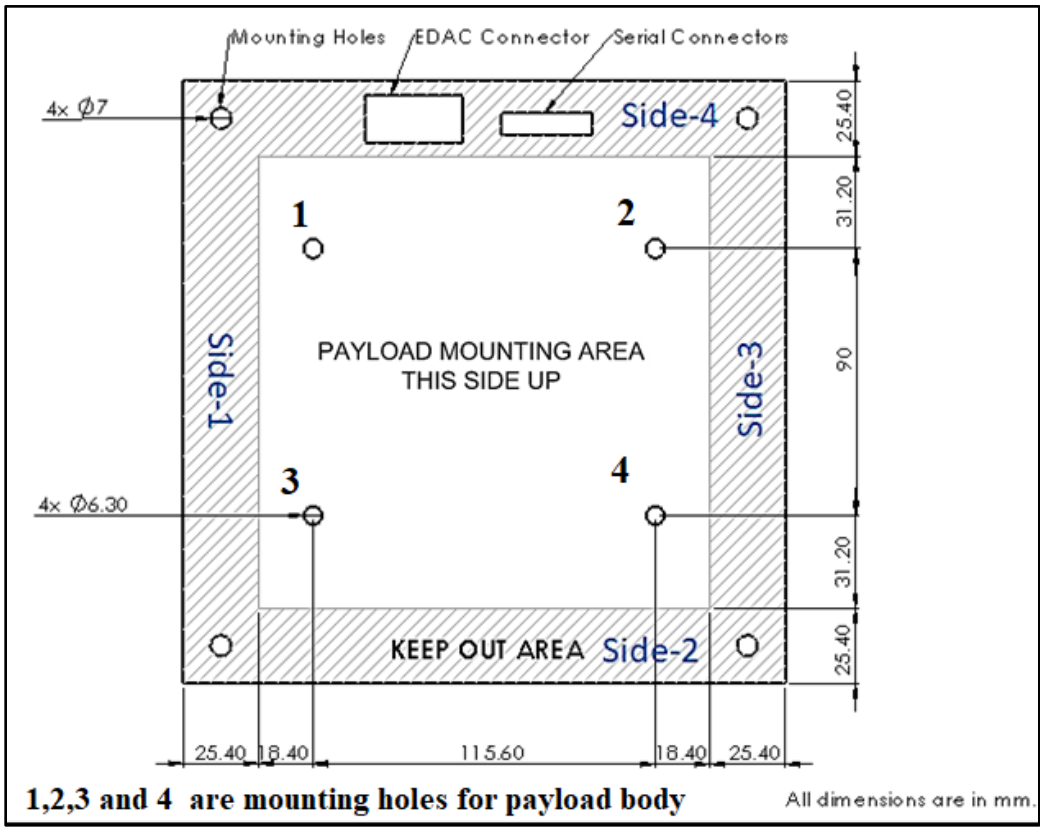


Fig. 5 Mounting Plate for small payload (Courtesy: HASP Version 02.17.09 [9]) http://laspace.lsu.edu/hasp/documents/public/HASP_Interface_Manual_v21709.pdf

1.5 Electrical Design

A block diagram of the circuit is shown in fig. 6 (a).

Several sections of the circuit diagrams are <u>provided in Appendix A (2)</u>. Refer to Fig. 16 (1) to (10) on pages59 to 66 for additional details of the circuits.

Two identical microcontroller PCBs are fabricated. One PCB will be used for the payload, whereas the other PCB will be used to stimulate the software and backup.

The microcontroller circuit was designed by Jonathan earlier and then redesigned and refabricated by Ken, Brittany, Chris, Miguel, Dustin and Colin during the previous flights.

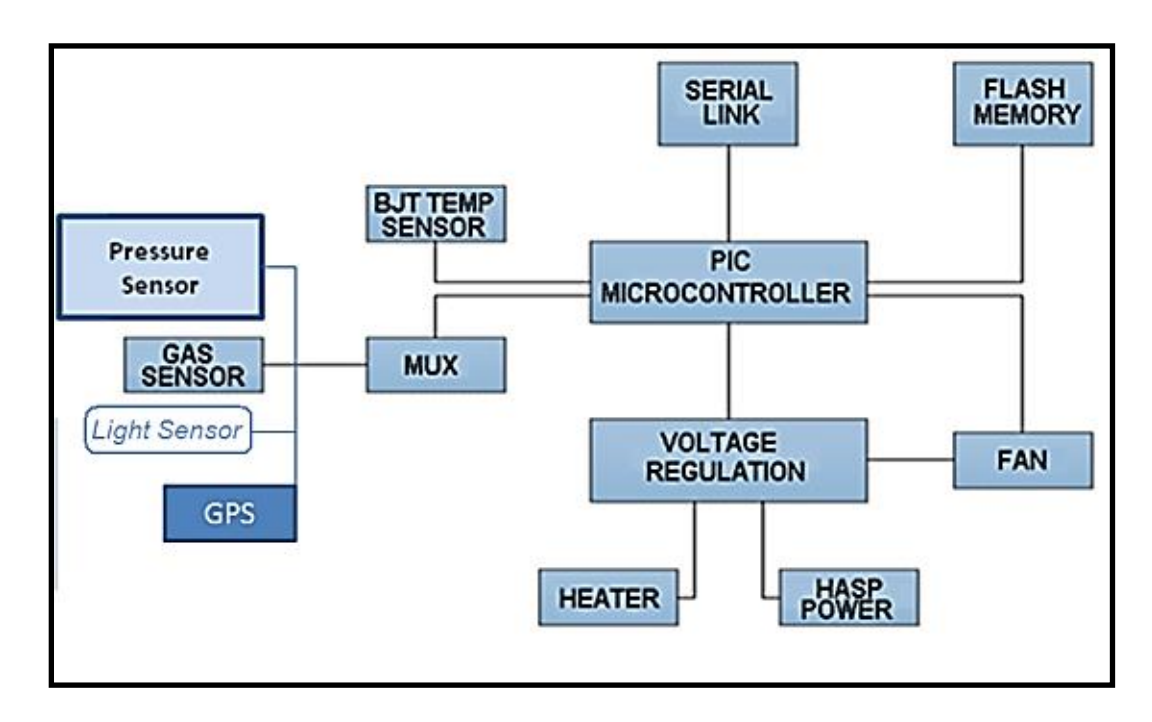


Fig. 6(a) Block diagram of the payload circuit.

1.6 Thermal Control Plan

Preliminary heat transfer calculations using equation (1) and heat transfer showed that the onboard sensor heater was adequate to maintain the sensor under nominal conditions. An additional exploration of the effects of temperature on component integrity is ongoing and is part of the investigation. These initial estimations utilized the proposed materials for the walls, and a minimum temperature of -60 °C (333 K or 140°F) and a general operating temperature of 15 °C (288 K or 59 °F) (determined from altitude variation from 0 km to 36 km shown in the modified altitude profile (Fig. 7).

Heat Transfer =
$$q = m(\Delta T) Cp$$
 (1)

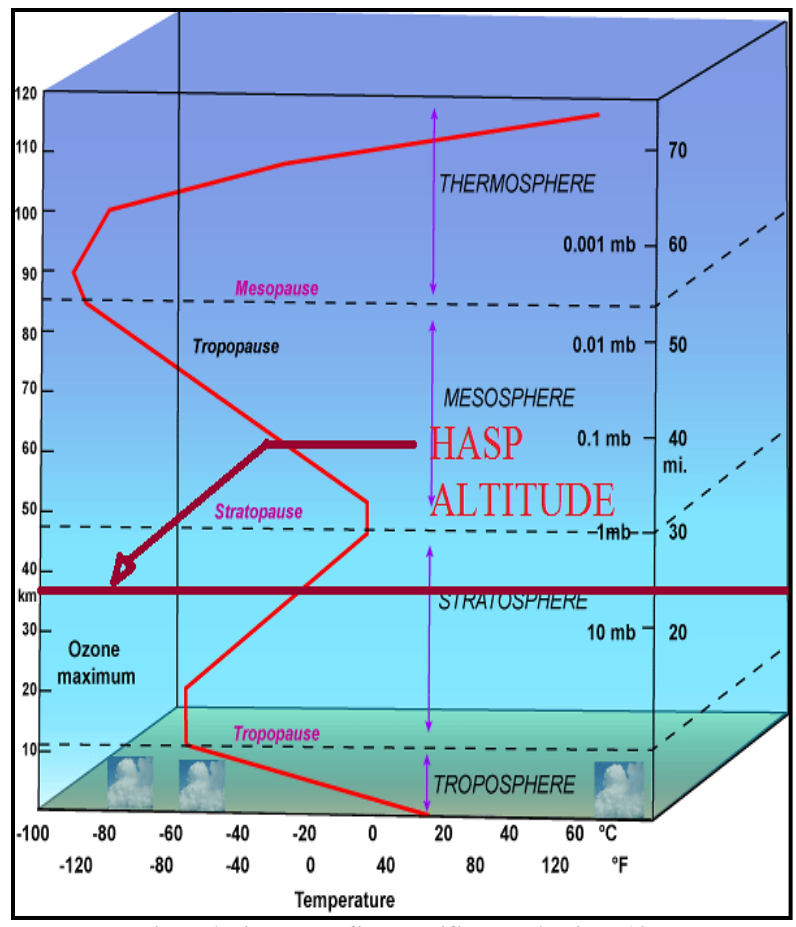


Fig. 7 Altitude profile modified by Atkins [10].

Our previous payloads exhibited good thermal stability. The payload body has better thermal stability against conduction and convection of heat in the temperature range -50 °C to 70 °C (= 223 K to 343 K) under high- and low-pressure conditions. We will attempt to further improve the thermal stability of the payload. As mentioned in our objectives, the outer surface of the payload body was covered by a thermal blanket made of an aluminized heat barrier with an adhesive backed (Part No. 1828) (www.PegasusAutoRacing.com) to improve thermal stability. The highly reflective surface of the material can withstand radiant temperatures more than 1000° C. This thermal blanket minimizes the variation in the internal electronic temperature conditions. The temperature of the ozone sensors was controlled in the range of $302 \pm 6^{\circ}$ K using an on-off controller, a polyimide flexible heater (MINCO make), and a temperature sensor TMP 36). We may replace the aluminum body of the payload with fiberglass, carbon composite, or alloy body to reduce weight and improve thermal stability.

The variation in temperature of three ozone sensor boxes #1, 2, and 3 with flight time during the HASP 2023 flight is shown in fig.8(a). The temperature of the sensors was kept constant at $302\pm6^{\circ}$ K. The variation in the temperature of the ozone sensors in boxes #1, # 2, and # 3 with altitude is shown in fig. 8 (b).

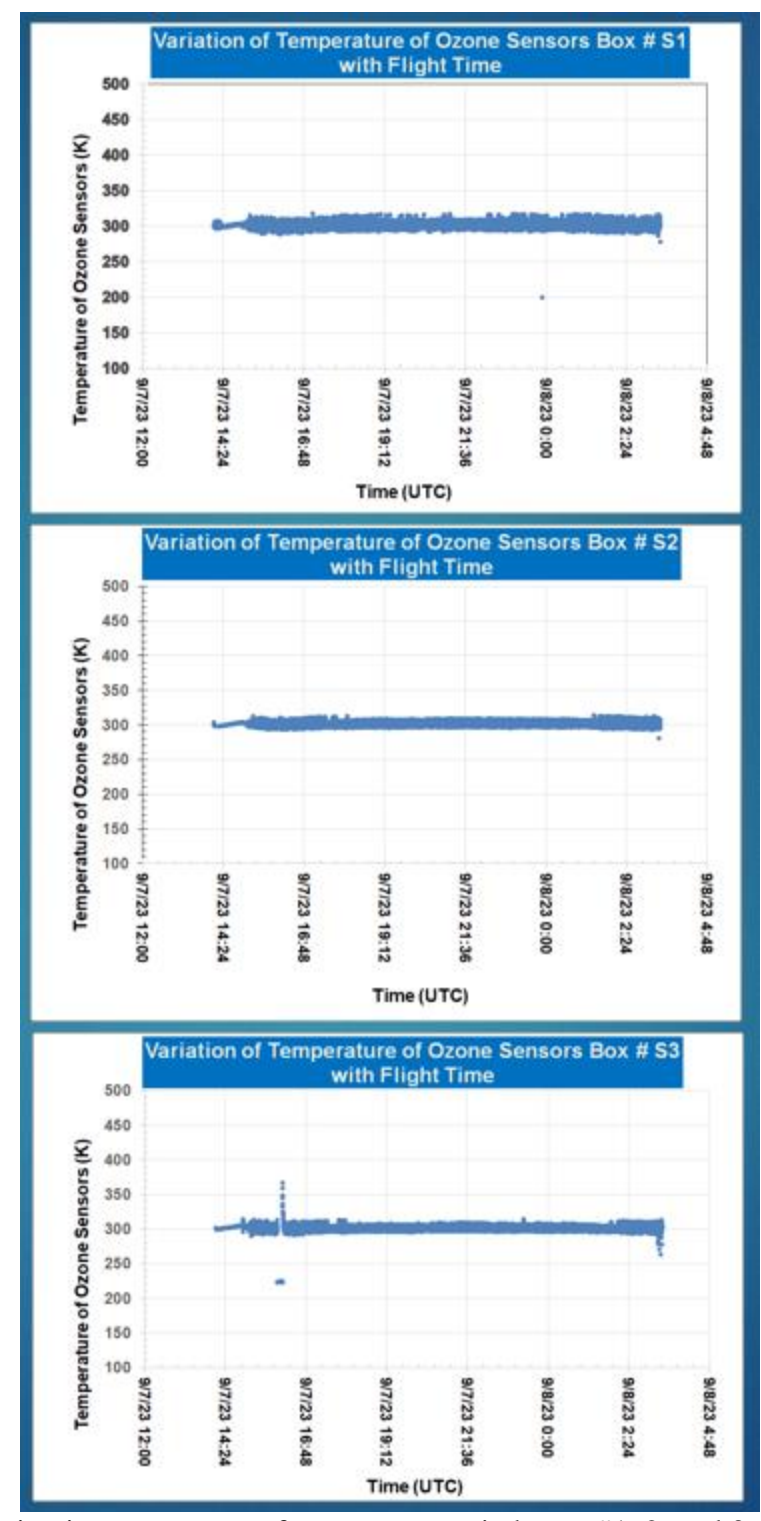


Fig. 8 (a) Variation in temperature of ozone sensors in boxes #1, 2, and 3 with time (UTC) during the HASP2023 flight.

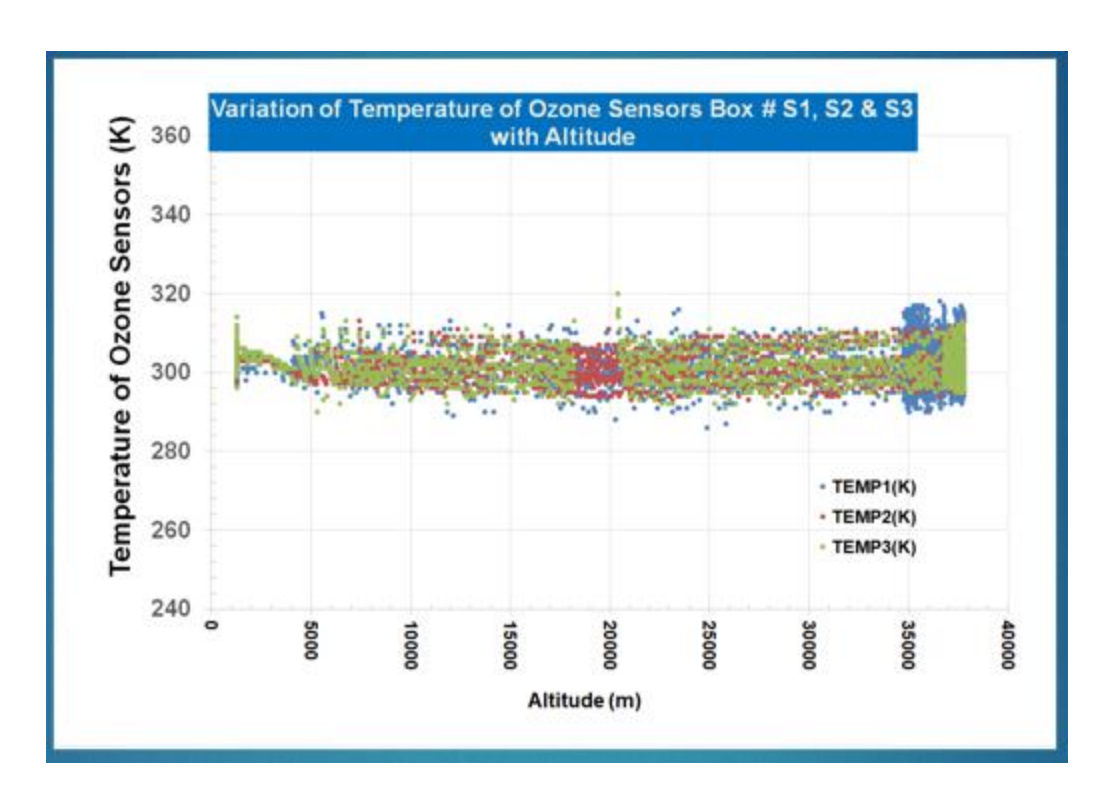


Fig.8 (b) Temperature of ozone sensor boxes #1, 2, and 3 during the HASP 2023 flight.

2. Team Structure and Management

2.1 Team Organization and Roles

Fig.9 shows a chart of team management. The listed work distribution is tentative and will be organized in January 2024.

HASP 2024 Team				
UNF	UND			
Dr. Nirmal Patel	Dr. Ron Fevig			
UNF Faculty Advisor	UND Faculty Advisor			
(1) Lovely Ramos (EE) (Team Leader)	Sam Reams and one more			
Administration, reporting and meeting, PCB, hardware, and	join later.			
sensors fabrication. Electrical power budget.	Space Studies			
(2) Dustin Leonard (EE) and (3) Patrick Buckley (EE)				
Space study, Sensor materials, Fabrication of sensors.				
Testing and calibration of sensors, test launch from				
Jacksonville.				
(4) Colin Ott (EE) and (5) Eliel Ortiz (EE)				
Payload body design, Fabrication, and integration, test				
launch from Jacksonville.				
(5) Corey Pare (ME) (Deputy Team Leader) and (6)				
Julian Rowe (ME)				
Helping Lovely with reporting work, Payload body design,				
fabrication, and integration. Weight and thermal budget.				
(7) Calla Taylor (ME) and (8) Diya Patel (EE)				
Payload body work, Software, 3-D printing, Sensors				
and Data Analysis.				
(9) Larry Ratcliff (EE) and (10) Aryan Patel (Computer)				
Programming, software, website and social media, travel,				
logistics, safety, and failure analysis.				

Fig.9 UNF-UND team

Faculty Advisors

Both Dr. Nirmal Patel (Faculty Advisor from UNF) and Dr. Ron Fevig (Faculty Advisor from UND) are involved in the development of sensors payload and participated HASP balloon flight since 2008. Both were jointly conducted through teleconference, video conference, text messages, and email communications with their team members regularly every month for the previous flights. This will continue for HASP 2024. Dr. Patel is mentoring students for the fabrication, testing, and calibration of nanocrystalline gas sensors, design and fabrication of payloads, data analysis, and improvement of software programs, whereas Dr. Fevig is mentoring students for the improvement of atmospheric studies and space applications. Both Dr. Patel and Dr. Fevig are citizens of the USA.

Demographic Information of Students

Lovely, Dustin, Colin, Cory, Calla, Aryan, and Julian worked as team members during the last HASP 2023 flight and will continue to work until HASP 2024. They launched two tethered balloons and two balloons during the annular solar eclipse on October 19, 2023. All team members

were citizens of the USA. Lovely is a dynamic Electrical Engineering student. She was studied under the guidance of Dr. Patel. She will continue to work as team leader. She will organize meetings, zoom video conference meetings with all members and faculty advisors, and communicate with HASP. She will take the lead for the integration and thermal vacuum testing of the payload at Palestine, TX, and pre-flight testing at Fort Sumner, NM. She will also be responsible for the flight operation plan, monthly reports, travel, and updating of the progress of work and any issues to both the advisors and the final science report. The demographic information of all the students is presented in Table 1.

Table-1 Demographic information of students

Name	Student Status	Race	Ethnicity	Gender	Disabled
Lovely Ramos N01486151@unf.edu 661-370-5383	UG-EE	Asian-Filipino	Non-Hispanic	Female	No
Dustin Leonard N01499961@unf.edu 904-885-0835	UG-EE	Caucasian/White	Non-Hispanic	Male	Yes
Colin Ott N01452568@unf.edu 267-272-9613	UG-EE	Caucasian/White	Non-Hispanic	Male	No
Cory Pare N01466895@unf.edu 954-849-7974	UG-ME	Caucasian/White	Non-Hispanic	Male	No
Calla Taylor N01508348@unf.edu 904-309-2222	UG-ME	Caucasian/White	Non-Hispanic	Female	No
Aryan Patel N01498500@unf.edu 904-982-5210	UG- Computer	Asian-American	Non-Hispanic	Male	No
Julian Rowe N01364794@unf.edu 904-566-4594	UG-ME	Caucasian-White	Non-Hispanic	Male	No
Larry Ratcliff N01505985@unf.edu 724-996-1830	UG-EE	Caucasian-White	Non-Hispanic	Male	No
Diya Patel N01520661@unf.edu 267-266-4221	UG-EE	Asian-American	Non-Hispanic	Female	No
Eliel Ortiz N01533226@unf.edu 253-678-4017	UG-EE	Black	Hispanic	Male	No
Patrick Buckley N01520839@unf.edu 904-347-1998	UG-EE	Caucasian-White	Non-Hispanic	Male	No
University of North Dak	cota				
Sam Reams	Graduate- Space Studies	Caucasian-White	Non-Hispanic	Male	No

2.2 Timeline and Milestones

The initial work breakdown schedule includes the basic tasks required of the HASP project, including the Proposal, Integration Plan, Integration Certification, Operation Plan, and Science Report. The proposed work-plan path is presented in the table.

Table-2 Timeline and Milestones

2024	UNF	UND		
January	Conceptual Design Review (CoDR) for sensors, electronic circuits, software, and payload. Reviewing science reports and issues of HASP2008 to 2023 flights.			
February	Preliminary Design Review (PDR) for sensors, electronic circuits, software, payload, integration of payload with HASP and data analysis.			
March	Critical Design Review (CDR) for sensors, ele payload, integration of payload with HASP and			
April	Designing of circuit board and programming. Fabrication and testing of sensor arrays, designing of payload body. Testing of a payload on tethered balloon from Jacksonville.			
May	Fabrication of circuit board and programming, modifications, if any Calibration of sensors and delivery of sensor arrays to UND for testing. Complete Payload Specification and Integration Plan (PSIP).			
June	Fabrication of sensors box and payload body. Reviewing HASP flights, data, and any issues.	Testing of circuit and sensor arrays. Integrating the circuits and the sensor arrays.		
July	Integration of circuit board and sensor box with the payload body. Development of protocols for communication of payload with HASP computer and RAW files to EXCEL file. Integration of sensor arrays in box. Integration of sensor boxes with payload body. Integration of PCB to payload and sensors box. Thermal vacuum testing at CSBF, Palestine, TX,			
August	Performing several tests on the payload at UNF. Flight operation plan, Testing payload, thermal vacuum test of payload and integration of payload with HASP platform. Submit Flight Operation Plane (FLOP).			
September	Pre-flight testing of payload, launching of payload from CSBF, Fort Sumner, NM and downloading data files, and data analysis work.			

October	Payload recovery, testing of sensor arrays and other components,			
	SEM+EDAX analysis of sensor arrays. Finding any issues and performing			
	failure analysis. Completing Data analysis.			
November	Data analysis and writing the final science report.			
December	Submission of the science report and planning for the next flight.			

Every month

- First Friday: To attend the HASP, Zoom Video Conference.
- Last Friday of submission of the monthly status report.

2.3 Anticipated Participation in Integration and Launch Operations

It is expected that at least three students from UNF and Dr. Nirmal Patel, faculty advisor from UNF, will travel to CSBF, Palestine, Texas, during the dates given by HASP for the integration of the sensor payload onto HASP. It is also expected that at least two students from the UNF and a faculty member (UNF) will travel to Ft. Sumner, NM for the launch of the HASP2024 payload on the dates given by the HASP and CSBF.

Anticipated Procedures

Prior to Integration:

- Testing and Calibration of sensor arrays
- The initial values for the data recorder are set.
- Place sensor arrays in appropriate payload slots
- Check the program and LED for status.

Integration:

- Mount payload module to HASP
- Connect HASP Power Connector as shown in Fig 10
- Connect HASP Serial Connection as shown in Fig 10

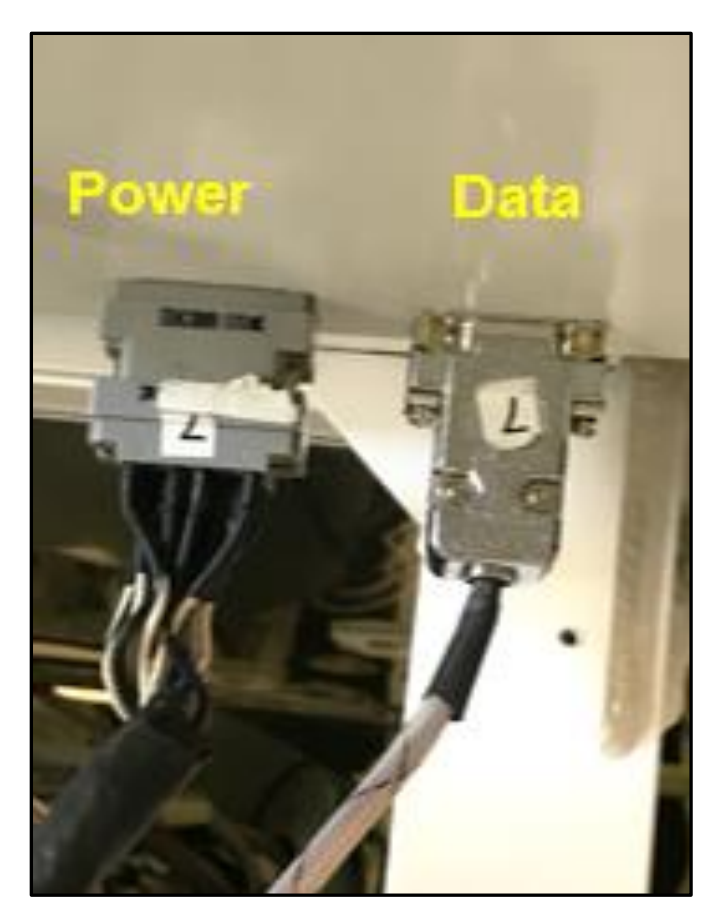


Fig. 10 Connection of power and data communication cables of HASP with payload (#7).

- The system was tested by recording the initial readings and ensuring that all the data were nominal.
- Troubleshoot

List all checks that determine successful integration.

- Communication and data checks were also performed.
- The command set was successfully executed.
- Monitor the system to ensure proper operation via real-time data stream of all sensor data readings, pressure, photo voltage of light sensors, and ambient temperature.

Pre-flight Operations and Testing

- The initial values for the data recorder are set.
- The sensors were placed in appropriate payload slots.
- Removes the protective cover from the payload body.
- The HASP power connector was connected.
- Connect HASP Serial Connection.
- The mass and size of the payload are checked.
- Test the thermal-low temperature and high-temperature tests and all commands.

- Test pressure and vacuum test
- Test 10g vertical and 3g horizontal vibration/impact test

Duration of Flight:

• We were flexible regarding the duration of the flight. A minimum of 6 to 8 h of flight during **the daytime** will be fine for us.

Flight Operations:

• Record values for resistance across the sensors

Post-Flight Operations:

- Examination of all parts of the payload. Working test of payload.
- Remove the PCB and sensor box from the payload. Test PCB with power and test sensor box
- Examine the sensor box for electrical testing, SEM+EDAX analysis, and failure analysis, if any.

3. Payload Interface Specifications

3.1 Weight Budget

The estimated weight budgets of various parts of the payload are listed in Table 3.

Table-3 Payload weight budget (without HASP Plate)

Item	Mass (g)	Uncertainty (g)	Measured / Estimated (g)
Three ozone sensors boxes including PCBs, fans, heaters, and boxes	600	6	600
Payload body, top plate, and thermal blanket	1000	10	1000
Microcontroller PCB with mounted components	300	2	350
Few ribbon cables, GPS and antenna, LEDs, UV light sensors, nuts, and bolts	350	10	350
TOTAL (g)	2250	16	2250

3.2 Power Budget

According to the instructions, on the EDAC 516 power connector, only pins A, B, C, and D are wired to the payload as +30 VDC power supply, and pins W, T, U, and X are wired to the payload as power ground to avoid failure of the power circuit or loss of payload. A voltage regulator is not necessary according to the initial tests despite the slightly higher +30 VDC at launch for the sensor; however, a voltage regulator and divider will be used for the peripherals. Fig. 11 (a) shows the EDAC516 receptacle pin layout.

The HASP provides power to the payload through the EDAC516 connector. Fig. 11 (b) shows the circuit diagram for interfacing the HASP mounting plate EDAC516 connector with the voltage regulation of the payload subsystems. Below is the switching power supply circuit used in previous payloads. It has been performed flawlessly. It is based on a National Semiconductor LM2956-3.3 switcher with ramp-up voltage capability provided by C11, R13, and R14. Thirty volts from the EDAC connector were provided via its four connections to a reverse-protection diode, D11. The current-limiting resistor R1 was in series with D11. The 30-volt supply is then reduced to 3.3 volts via the switching power supply U21 and supporting components.

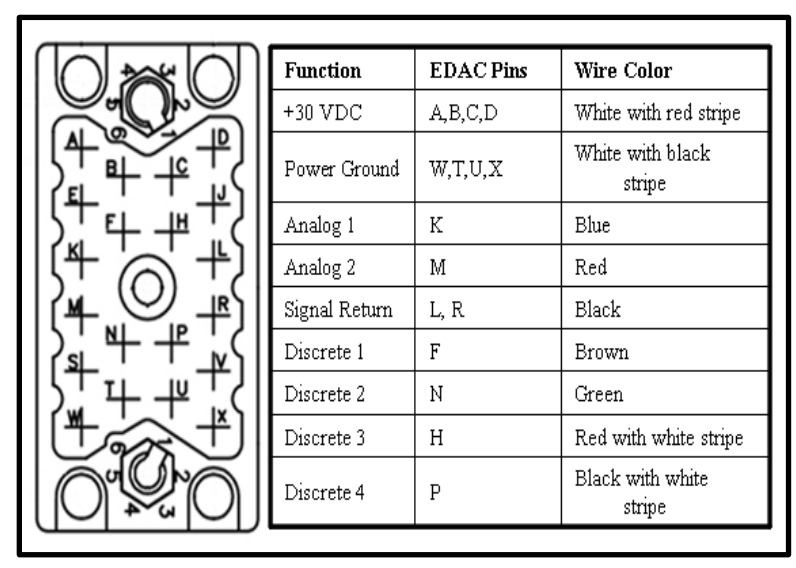


Fig. 11(a) EDAC516 receptacle pin layout (Courtesy: HASP manual).

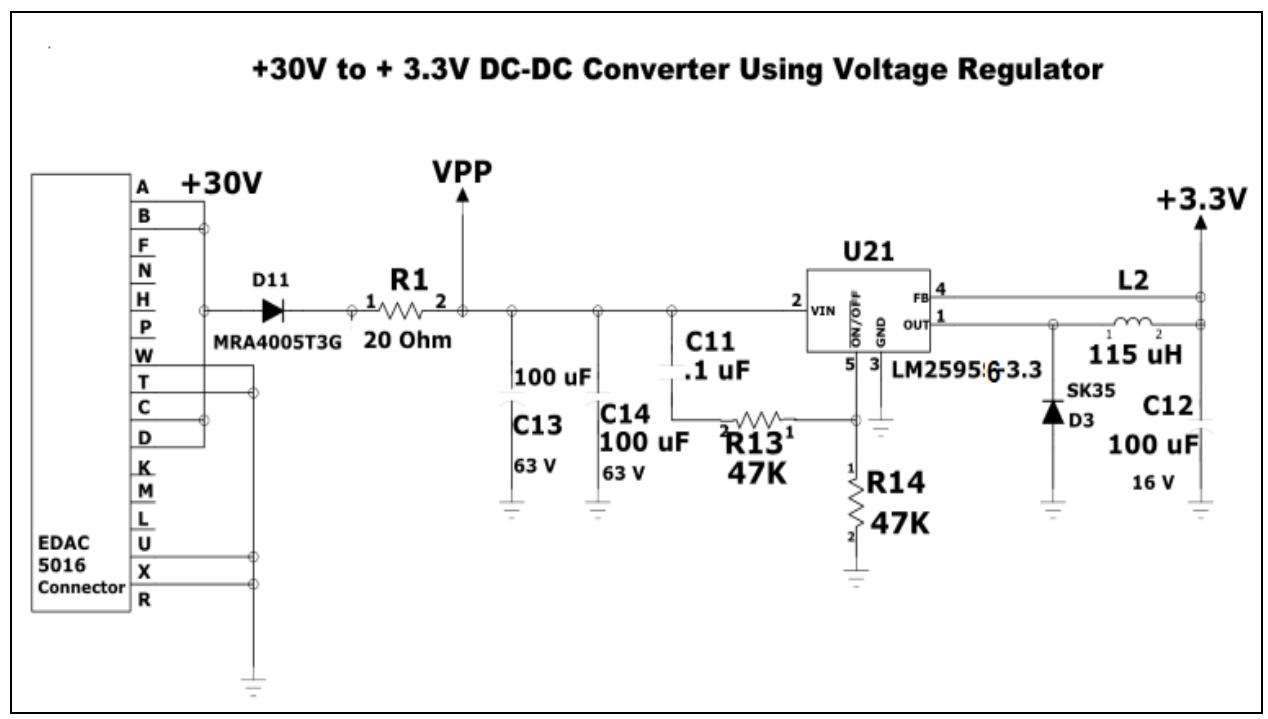


Fig. 11 (b) shows the EDAC 5016 interface of the mounting plate with the payload voltage regulation circuit.

The voltage applied to the payload during HASP 2023 flight is shown in fig.12 (a). The average applied voltage remained nearly constant at approximately 3300 mV.

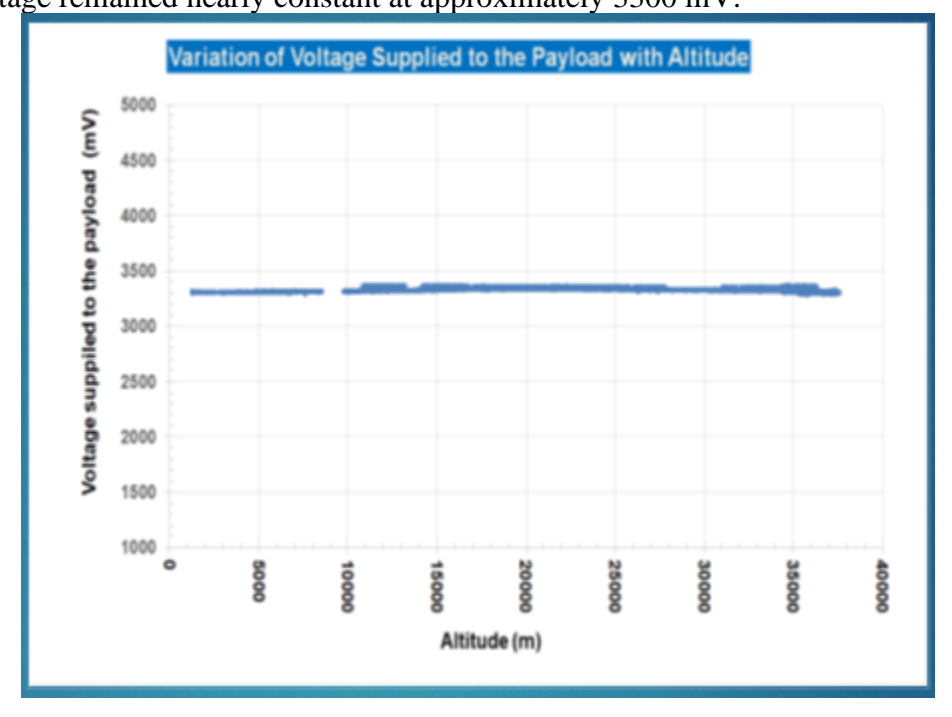


Fig.12 (a) Voltage applied to payload during HASP 2023 flight.

The current drawn by the payload during HASP 2023 flight is shown in fig. 12(b).

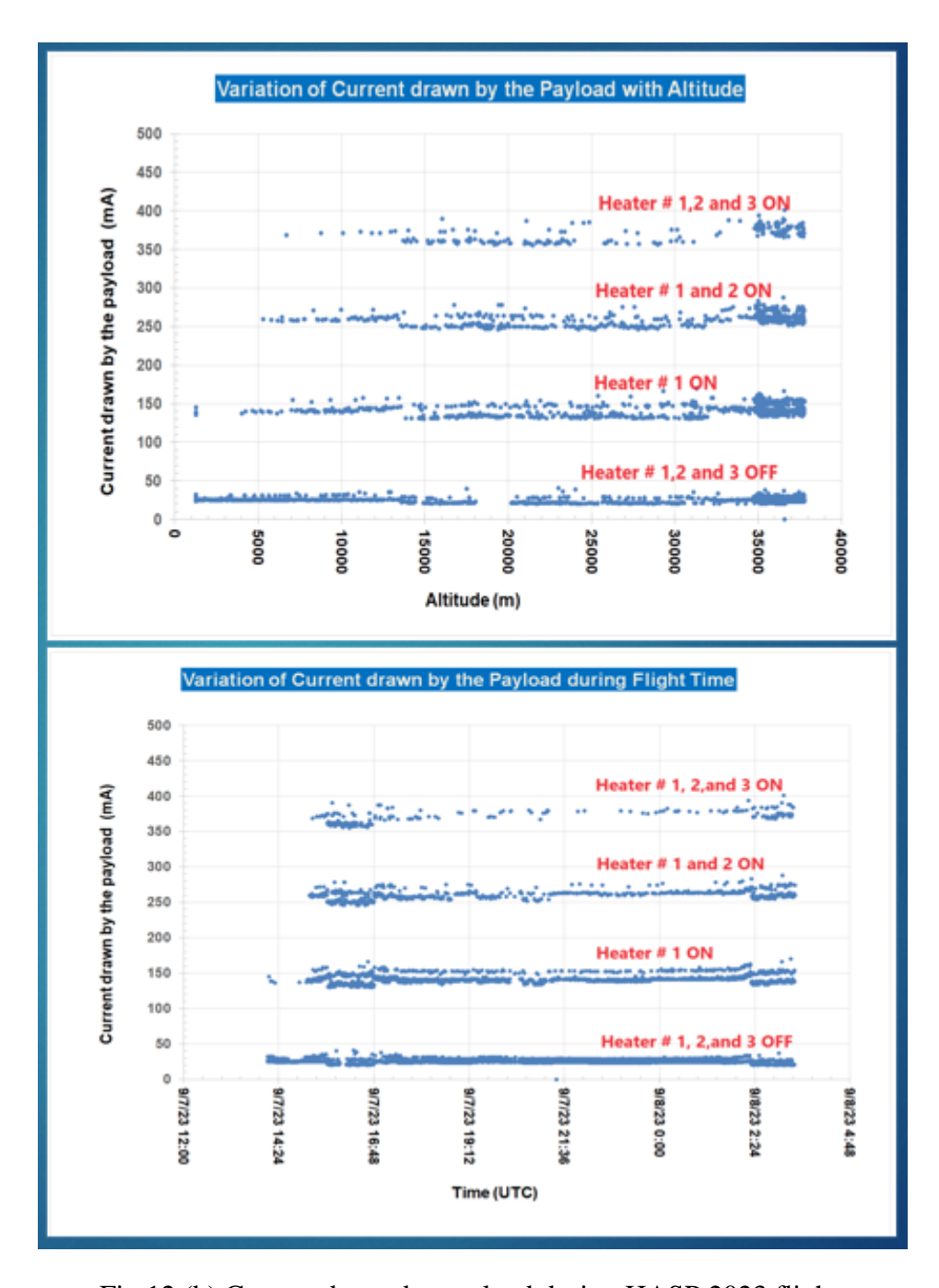


Fig.12 (b) Current drawn by payload during HASP 2023 flight.

The measured current drawn by the payload during the HASP 2023 flight at a payload voltage of 3.3 and HASP voltage of 30 V for the operation of the three heaters is listed in Table 4.

Table-4 Current Draw by the payload during HASP 2023 flight

Circuit Function	Current draw (mA)
Payload Power ON, but all heaters OFF	40±5
Payload Power ON and Heater #1 ON	150±20
Payload Power ON, Heater #1 and 2 ON	260±20
Payload Power ON, Heater #1, 2 and 3 ON	360±25

The power budget was maintained below the upper limit of the HASP requirements during the previous HASP 2023 flight. The 0.5Amps at 30VDC supplied by the HASP adequately accommodated the power requirements for the payload electronics, as well as the heater and fan for the sensor. The expected current and power generated by the payload are listed in Table 5.

Table-5 Expected Power budget of the payload for HASP 2024

Item	Current (A)	HASP Voltage (V)	Power (W)=	Uncertainty Power (W)
Payload Power ON + All heaters OFF	0.040	30.0	1.20	0.15
Payload Power ON + one heater ON	0.040+0.110 =0.150	30.0	4.50	0.15
Payload Power ON + two heaters ON	0.040+0.220 =0.260	30.0	7.80	0.15
Payload Power ON + three heaters ON	0.040+0.330	30.0	11.10	0.15
Maximum Total	0.370	30.0	11.10	0.30

Measured maximum current draw at 30 VDC: **0.40 A (when all heaters ON)**

The minimum power drawn by the payload will be about 1.20 ± 0.02 W, while maximum power drawn will be about 11.10 ± 0.30 W at 30V supply from HASP. Most of the time, the power drawn by the payload during the float will be less than 1.0 W. This expected power consumption is less than the 15 W limit for smaller payloads.

3.3 Downlink Serial Data

The payload module required RS232 HASP telemetry to send the status of resistance values to the ground. A data-recording unit is included with the master controller on the PCB if the telemetry link fails. The DB9 connector (Fig.13) is required for the telemetry system of telemetry system so that the data can be sent to the base station via the RS232 link. The RS232 link operates at 2400 baud using the standard RS232 protocol with eight data bits, no parity, one stop bit, and no flow control. A standard packet will contain the information formatted vis-à-vis the Student Payload Serial Connection section of the HASP-Student Interface Document.

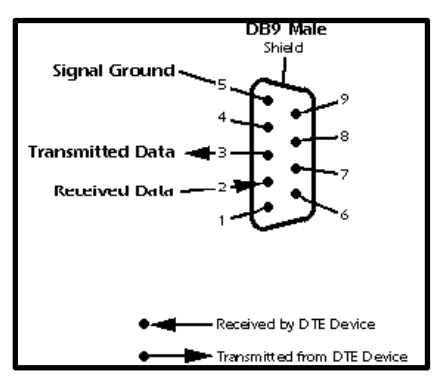


Fig. 13 DB9 pin diagram (Courtesy: HASP manual)

Downlink Telemetry Specifications

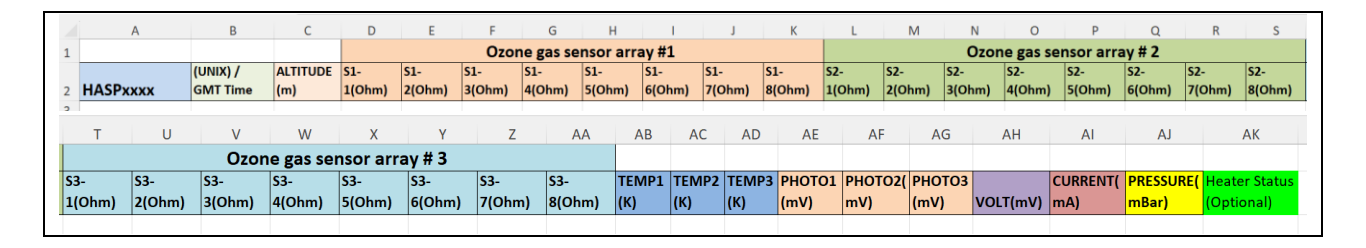
- (a) Serial data downlink format
 - Packetized- Record +/- 232 bytes transmitted in 5 s intervals.
- (b) Approximate serial downlink rate: 372 bps
- (c) Table-6 shows the information about serial data records, including the record length and information contained in each record byte. Total record length: 238 bytes

Table-6 (a) Data record length

Byt	te	#	Description	Example	Units	126	- 1	31	Sensor 3-1	.01495	ohms
1 -	-	4	Packet Sync	HASP	n/a	132	- 1	37	Sensor 3-2	,01652	ohms
5 -	-	8	GPS Source	XGPS	n/a				Sensor 3-3	.01669	ohms
9 -	-	23	Time stamp	,1407604205.265	sec	144			Sensor 3-4	,01748	ohms
24 -	-	29	Altitude	,38044	m					,	
30 -	-	35	Sensor 1-1	,01067	ohms	150		-	Sensor 3-5	,01720	ohms
36 -	-	41	Sensor 1-2	,01390	ohms	156	- 1	61	Sensor 3-6	,01619	ohms
42 -	-	47	Sensor 1-3	,01438	ohms	162	- 1	67	Sensor 3-7	,01506	ohms
48 -	-	53	Sensor 1-4	,01248	ohms	168	- 1	73	Sensor 3-8	,01441	ohms
54 -	-	59	Sensor 1-5	,01282	ohms	174	- 1	79	Temp 1	,00298	K
60 -	-	65	Sensor 1-6	,01450	ohms	180	- 1	85	Temp 2	,00309	K
66 -	-	71	Sensor 1-7	,01358	ohms	186	- 1	91	Temp 3	.00297	K
72 -	-	77	Sensor 1-8	,01060	ohms	192	- 1	97	Photovoltage 1	.00460	mV
78 -	-	83	Sensor 2-1	,01623	ohms			_	Photovoltage 2	,00464	mV
84 -	-	89	Sensor 2-2	,02874	ohms			_		,	
90 -	-	95	Sensor 2-3	,02999	ohms	204		_	Photovoltage 3	,00467	mV
96 -	-	101	Sensor 2-4	,01820	ohms	210	- 2	215	CPU Temp	,00304	K
102	-	107	Sensor 2-5	,01993	ohms	216	- 2	221	Power Rail Voltage	,03317	mV
108	-	113	Sensor 2-6	,02956	ohms	222	- 2	227	Power Rail Current	,00148	mA
114	-	119	Sensor 2-7	,02812	ohms	228	- 2	233	Pressure	,00117	mBar
120	-	125	Sensor 2-8	,01371	ohms	234	- 2	238	Heater Status	,1101	n/a

The standard RS-232 connectivity rate for a small payload is 1200 baud. We will certainly attempt to remain within the limits of this time by improving our software program and hardware.

Table 6(b) Data recorded on the EXCEL worksheet.



- (d) Number of analog channels used:0.
- (e) The number of discrete lines used :0.
- (f) Are there any onboard transmitters? **No.**
- (g) Other relevant downlink telemetry information. Not Applicable.

3.4 Uplink Serial Commanding

Command uplink capability required: Yes.

- (h) If so, the commands are uplinked at regular intervals, that is, **No.**
- (i) How many commands do you expect to uplink during the flight (can be an absolute number or a rate, i.e., *n commands per hour*): one command per hour maximum.
- (j) Provide a table of all commands that you will link to your payload.

The proposed commands are listed in table-7 (a) and (b). Any changes in the list are updated at the time of PSIP and FLOP.

Table 7 (a): List of Commands in general

		Cmd.	Checksu	
#	Command Description	Code	m	Confirmation/Notes
1	Reset	0x71	0x31	"HELLO" upon reset
				"ERASING FLASH""
2	Erase data in flash	0x72	0x32	COMPLETE"
3	Upload data in flash	0x73	0x33	"NO DATA"
4	n/a	n/a	n/a	n/a
5	Master Heater Override Switch On	0x75	0x35	Heater Status (default)
6	Master Heater Override Switch Off	0x76	0x36	Heater Status
7	On Board Data Logging On	0x77	0x37	Data (default)
8	On Board Data Logging Paused	0x78	0x38	Data empty
9	Stream UNF GPS data	0x79	0x39	"UGPS"
10	Stream HASP GPS data	0x7A	0x3A	"HGPS"

Table 7 (b) List of Uplink Commands

Command Name	2-Byte Command Hex Code	Command Description
RESET	7131	Reset System
HEATER SWITCH_OFF	7535	Turn Master Heater Switch OFF. The main heater switch is disable. All three heaters will remain switch OFF.
HEATER SWITCH_ON	7636	Turn Master Heater Switch On (default). The main heater switch is enabled and thus each individual heater can turn ON or OFF as needed by the temperature controller.
UBLOX_STREAM	7939	Stream GPS via Embedded GPS (default).
HASP_STREAM	7A3A	Stream GPS via HASP GPS

(k) Other relevant uplink command information. None

3.5 Analog Downlink: None.

3.6 Discrete Commanding: None

3.7 Payload Location and Orientation Request

The requested smaller payload should be oriented on the side away from any solar cell to avoid disparate solar thermal radiation. There should not be any obstacle for air circulation into the

payload or any shadow of other payloads. We would like the position of the payload (#7) on the HASP to be the same as that on previous flights. Fig. 14 (a) and (b) show the desired payload location on the HASP.

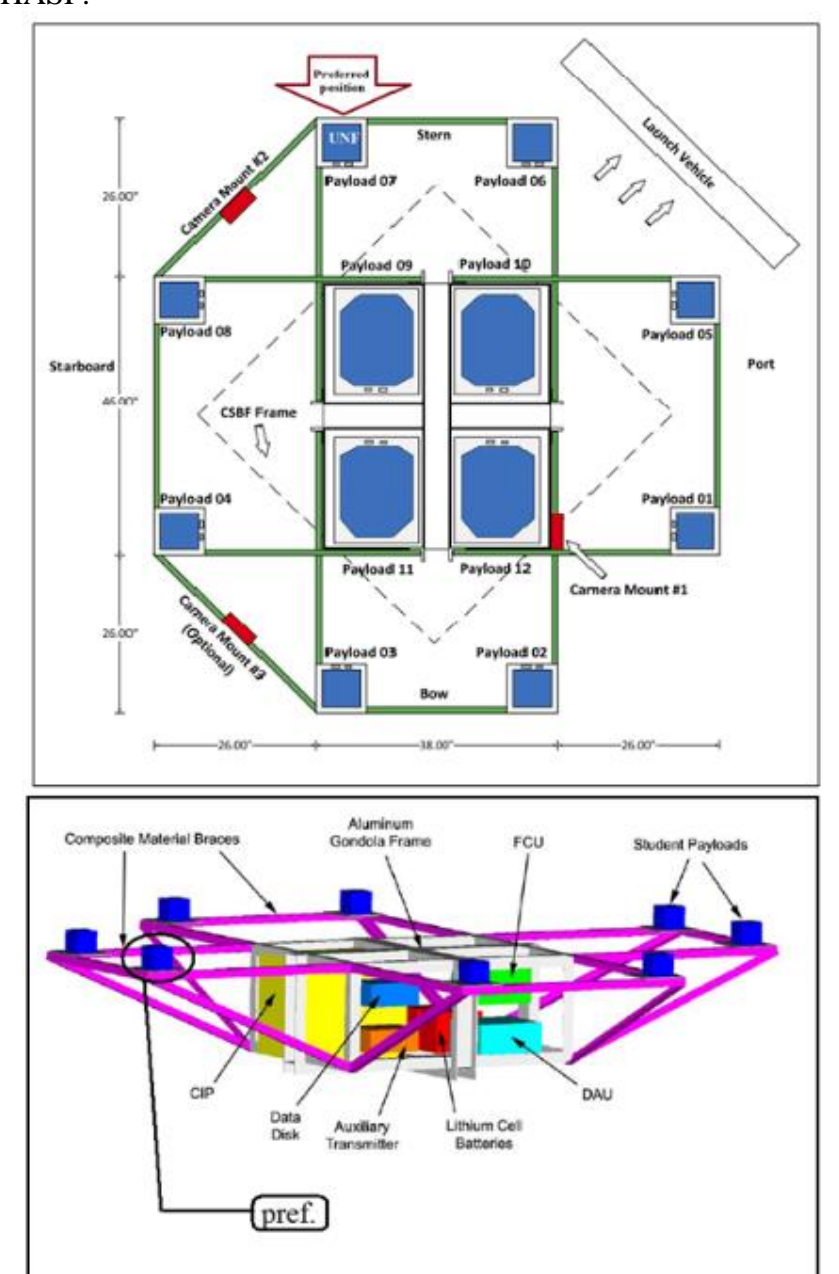


Fig. 14 (a) Top view (b) side view proposed HASP Configuration Dr. Guzik and Wefel [11]

http://laspace.lsu.edu/hasp/documents/public/HASP_Interface_Manual_v21709.pdf

3.8 Special Request

We request the HASP to provide us with GPS strings from the HASP gondola every 2 s in case of failure of our payload GPS.

4 Preliminary Drawings and Diagrams

Please refer to Appendix A (1) pages 42 to 58 for mechanical drawings and Appendix-A (2) pages 59 to 66 for electrical drawings. Any changes in the drawing are reported in the PSIP and FLOP documents.

5. References

- [1] Perry J. Samson, "Nocturnal Ozone Maxima" Atmospheric Environment, Vol.12 (1978) 951-955.
- [2] A. Mavrakis, H. Flocas, E. Mavromatidis, G. Kallos, G. Theoharatos and A. Christides, "A Case of Nightime High Ozone Concentration over the Greater Athens Area", Meterologische Zeitschrift, Vol. 19, No.1 (2010) 035-045.
- [3] R. San Jose, A. Stohl, K. Karatzas, T. Bohler, P. James and J.L. Perez, "A Modelling Study of an Extraordinary Nighttime Ozone Episode over Madrid Domain". Environmental Modelling & Software 20 (2005) 587-593.
- [4] Nanocrystalline indium tin oxide sensors and arrays. U.S Patent No. 9,606,078 B2, March 28, 2017.
- [5] Nanocrystalline Indium Tin Oxide Sensors and associated methods of use. U.S. Patent No.:10,823,690 B2 Nov. 3. 2020.
- [6] Quartz crystal microbalance with nanocrystalline oxide semiconductor thin films and method for the detection of vapors and odors, including alcoholic beverages, explosive materials, and volatilized chemical compounds.

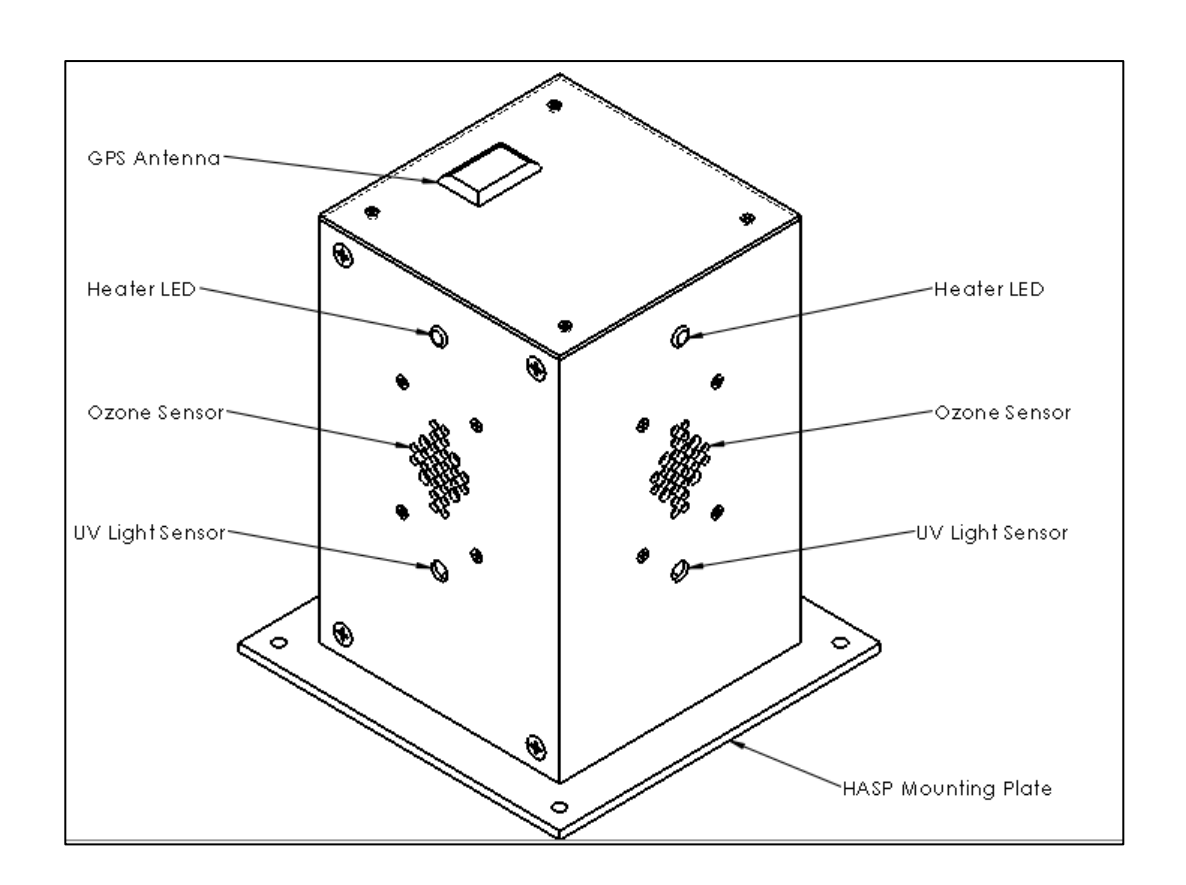
 U.S Patent No. 7,930,923 B2, April 26, 2011
- [7] Solid-State Sensors Behavior in Reduced Pressure Environments Demonstration Using an Experimental Indium Tin Oxide Ozone Gas Sensors for Ozone Sounding; Nathan Ambler, Ronald Fevig and Nirmal Patel, Proceedings of 59th International Astronautical Congress, Glasgow (Sept 29-Oct 3, 2008), C2. I.17
- [8] Hansford, Graeme, et al. "A low cost instrument based on a solid state sensor for balloon-borne atmospheric O₃ profile sounding." Journal Environmental Monitoring (2005): 158-162.
- [9] HASP Student Payload Interface Manual, Version 02.17.9 http://laspace.lsu.edu/hasp/documents/public/HASP_Interface_Manual_v21709.pdf
- [10] Atkins, Noel. Survey of Meteorology. 10 November 2007
- [11] Guzik, T. Gregory and John P. Wefel. "The High Altitude Student Platform (HASP) for Student-Built Payloads 35th COSPAR Scientific Assembly. Houston, Texas, 2004. 1-8.



HASP 2024

Appendix-A (1)

Mechanical Drawings of the Payload Body



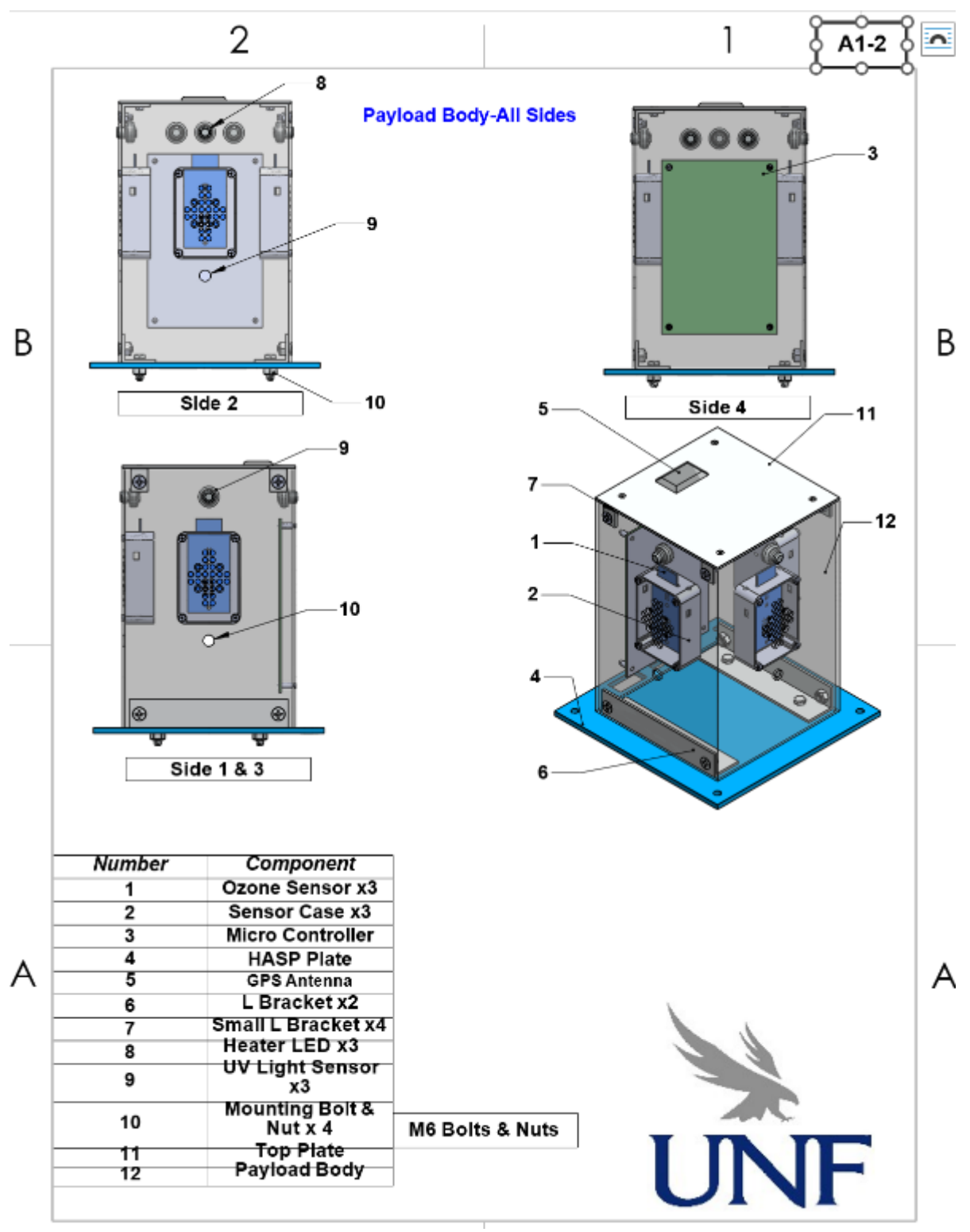


Fig. 15(a) Payload body all sides.

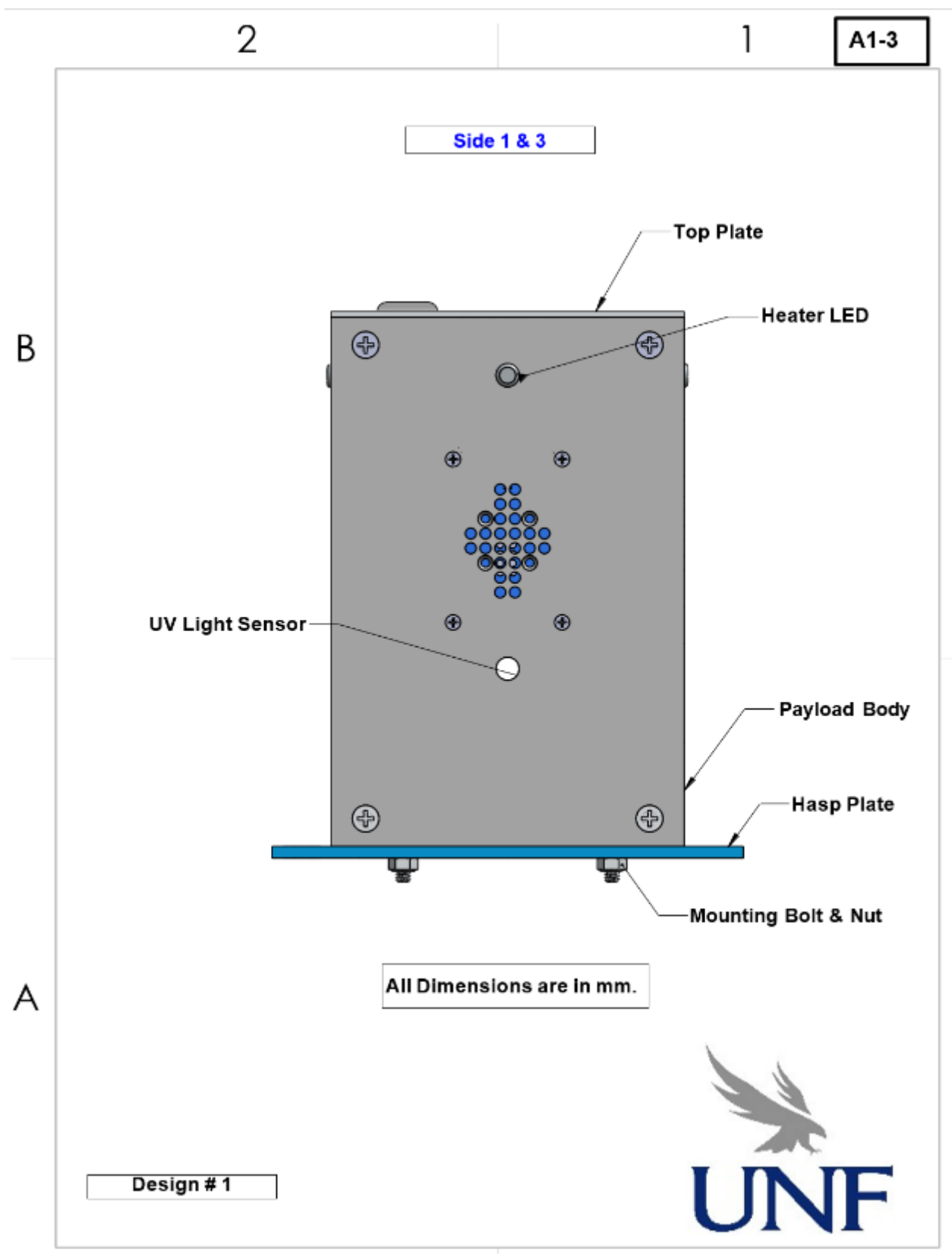


Fig. 15(b) Sides 1 and 3 outside.

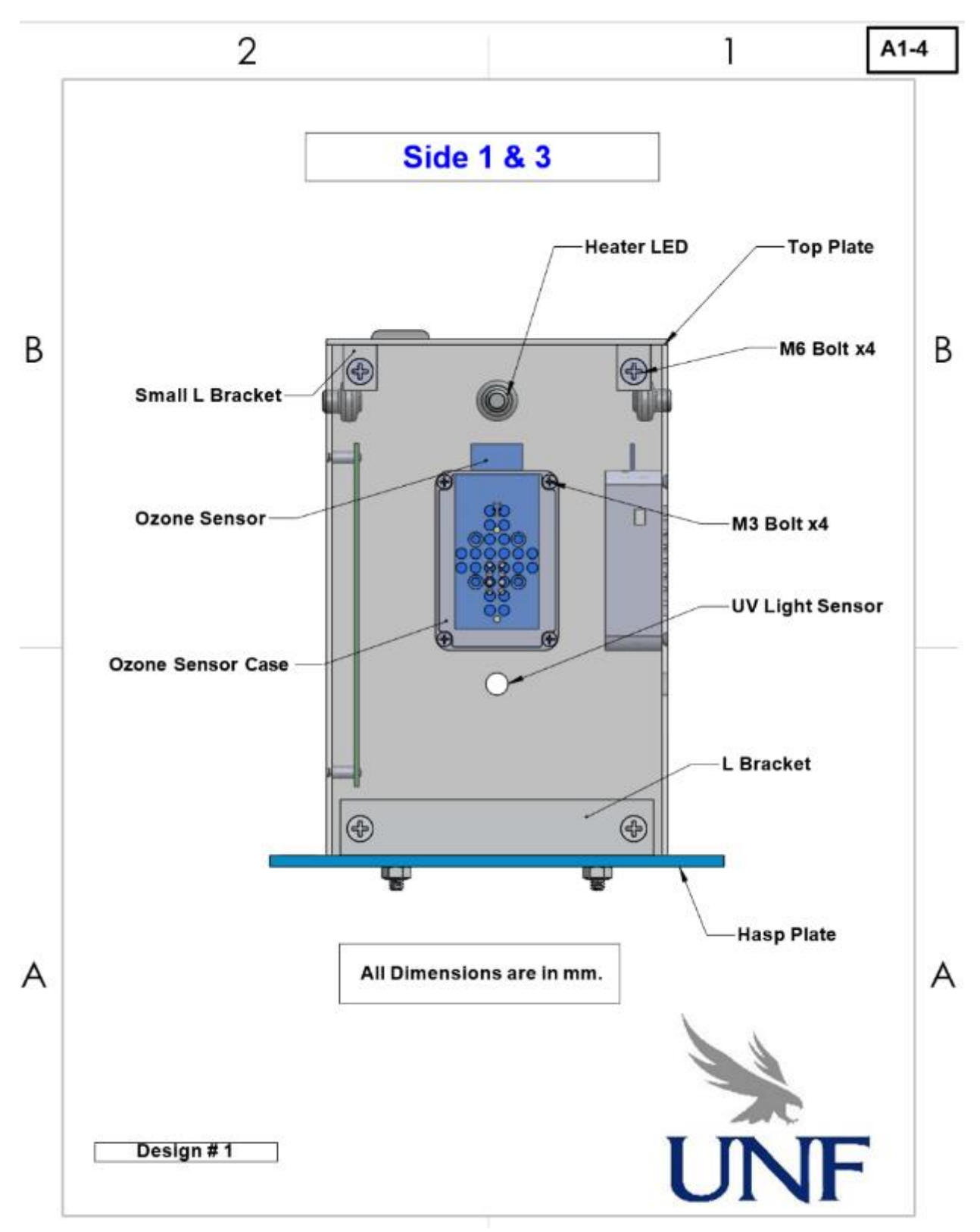


Fig. 15(c) Sides 1 and 3

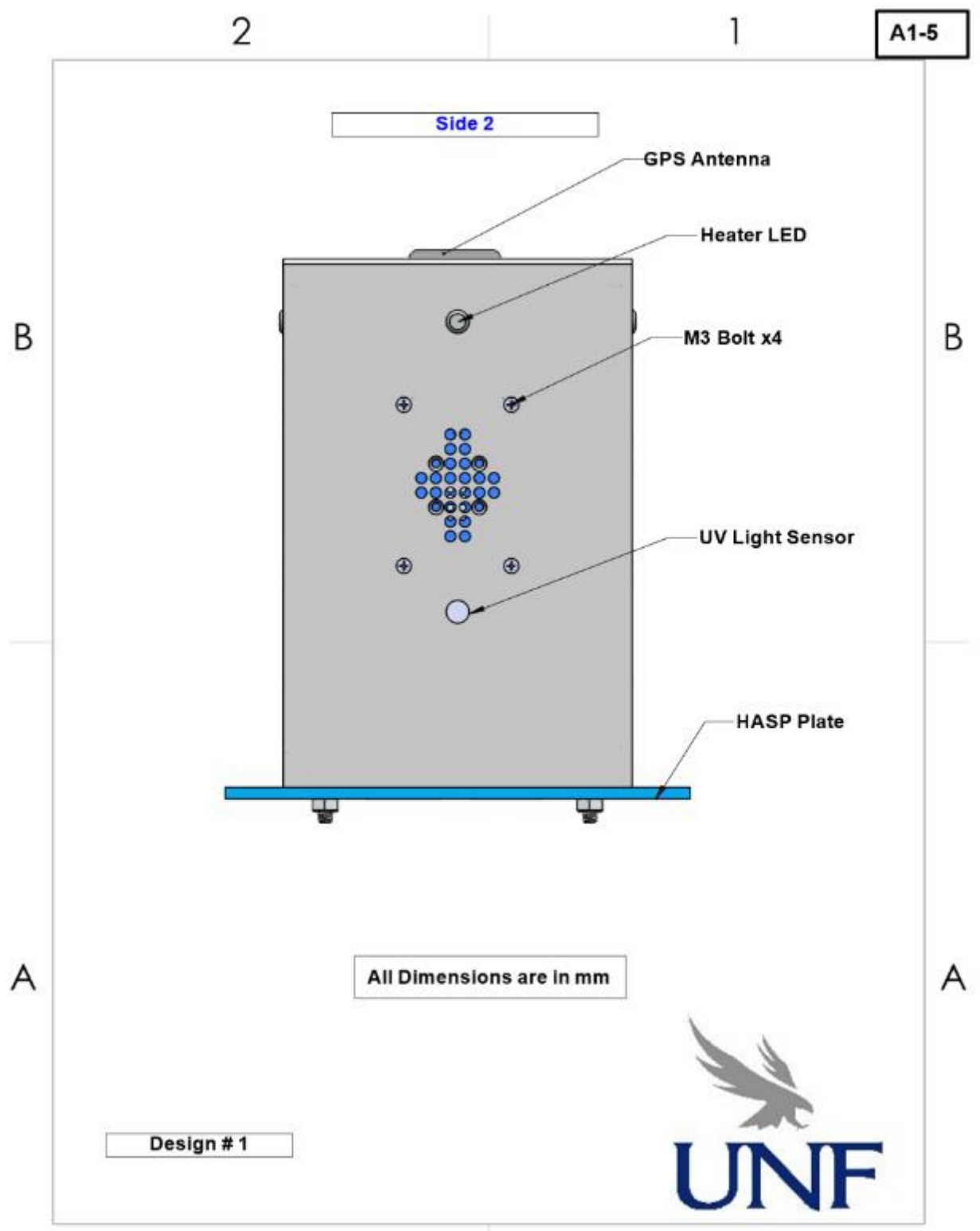


Fig. 15(d) Side 2 Outside.

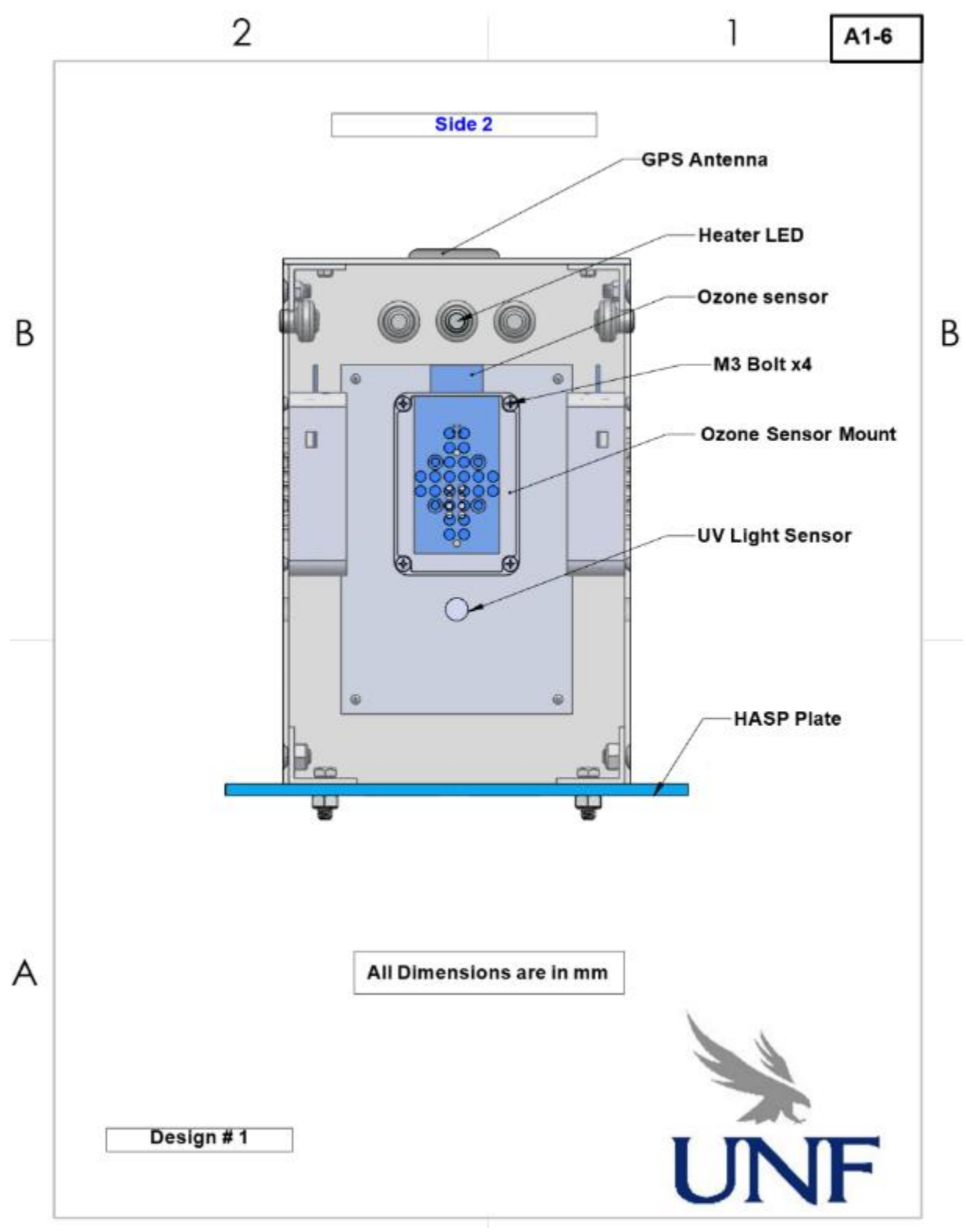


Fig. 15(e) Side 2 Inside.

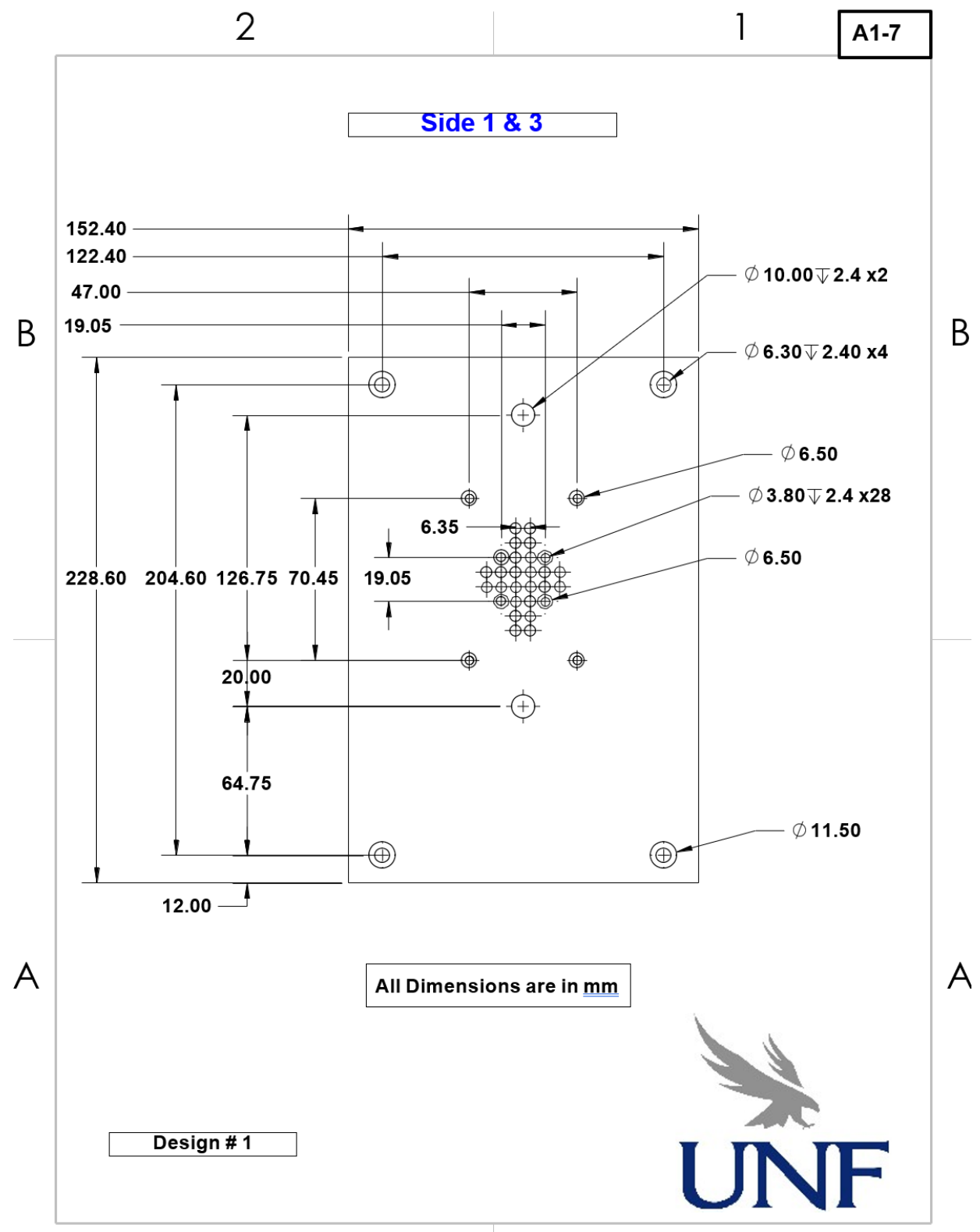


Fig. 15(f) Side 1 & 3 Holes.

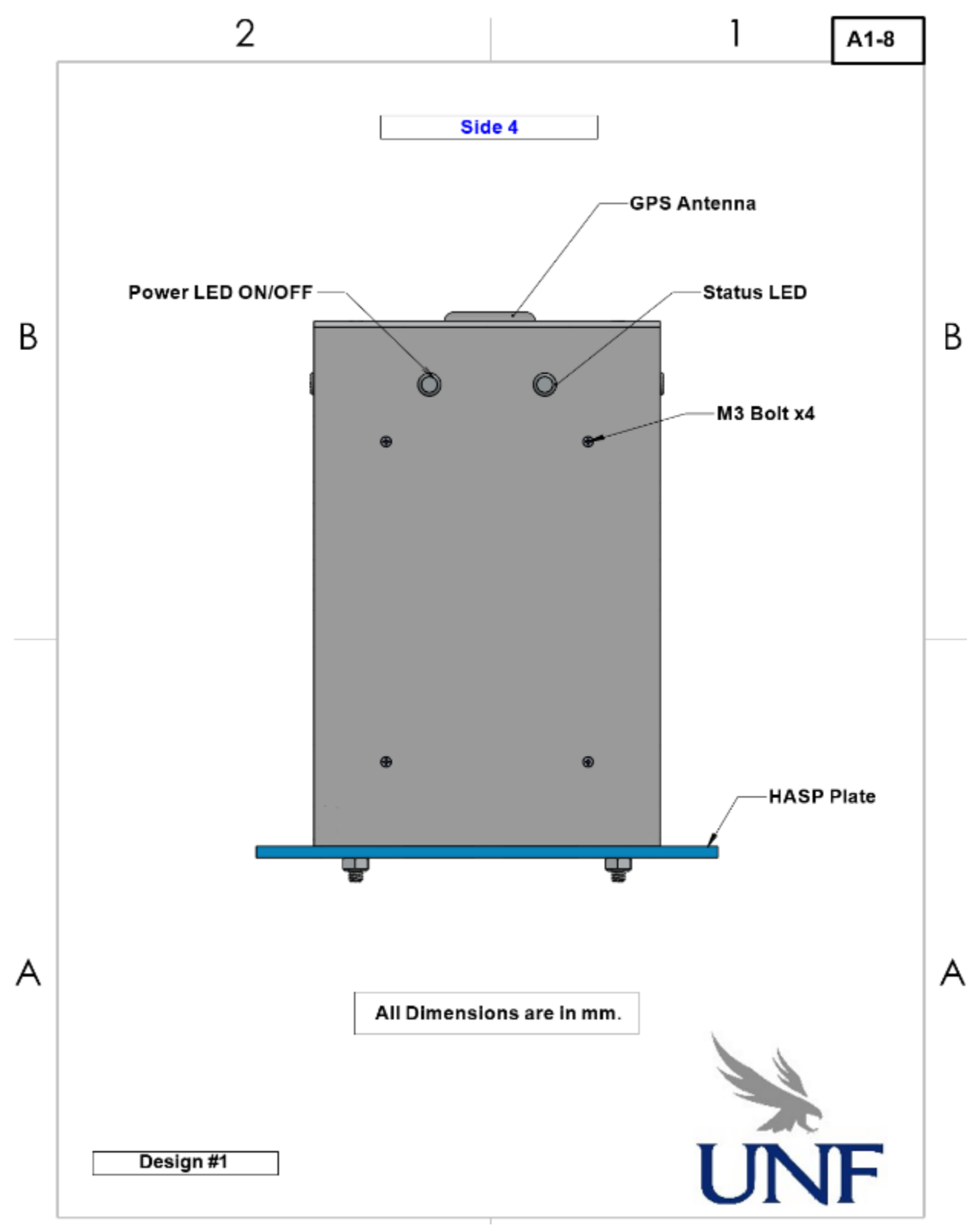


Fig. 15(g) Side 4

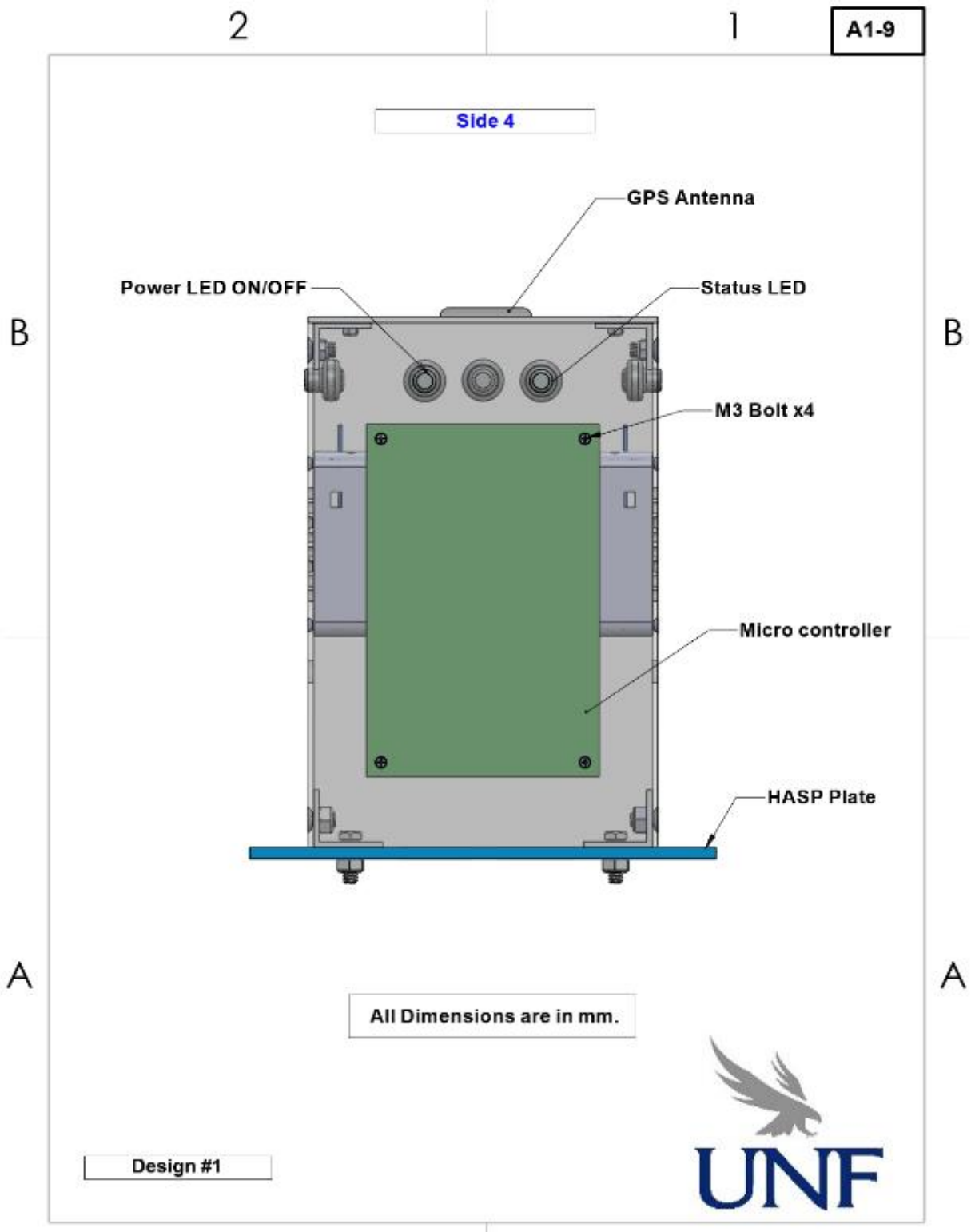


Fig. 15(h) Side 4 Inside.

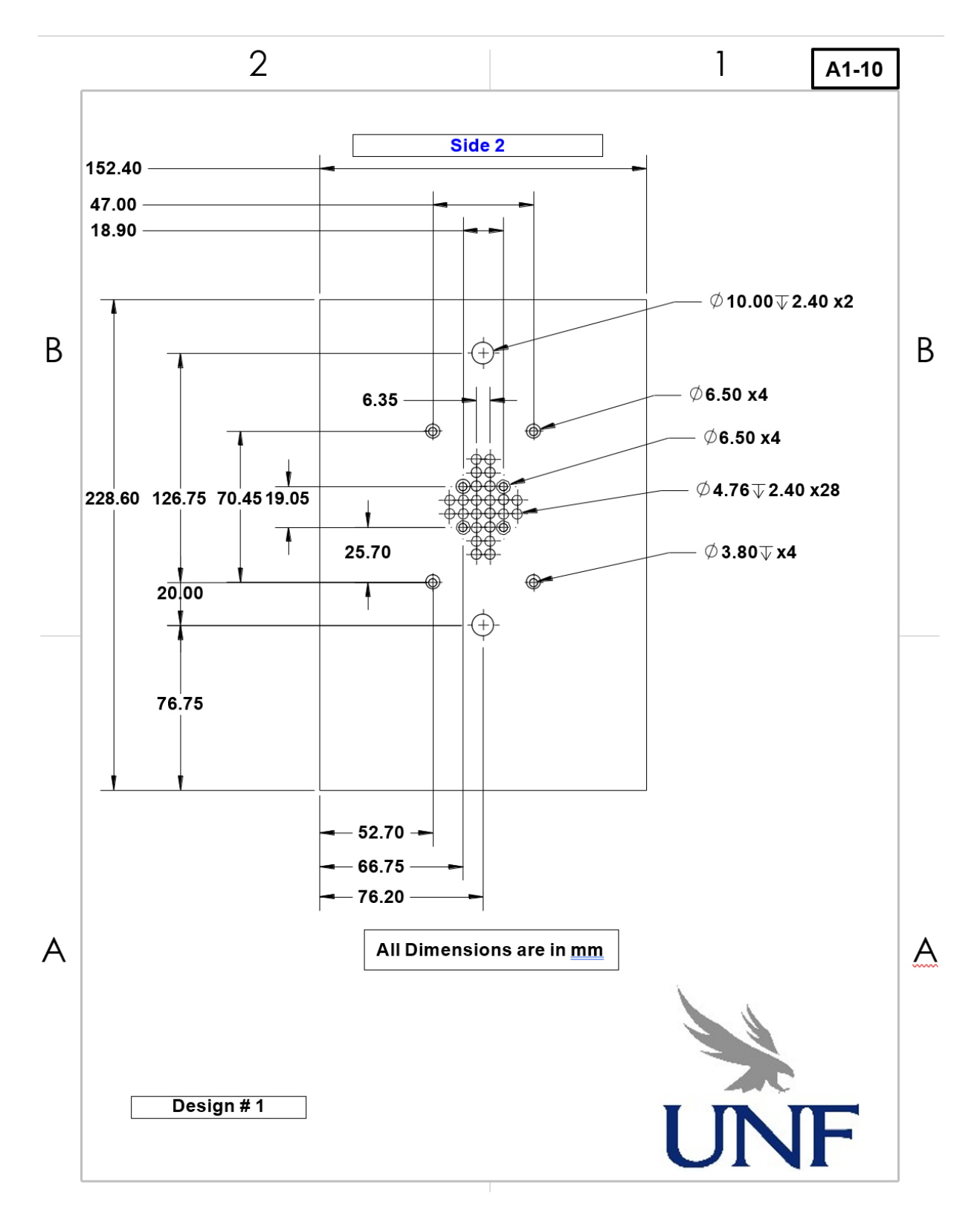


Fig. 15(i) Side 2 Holes.

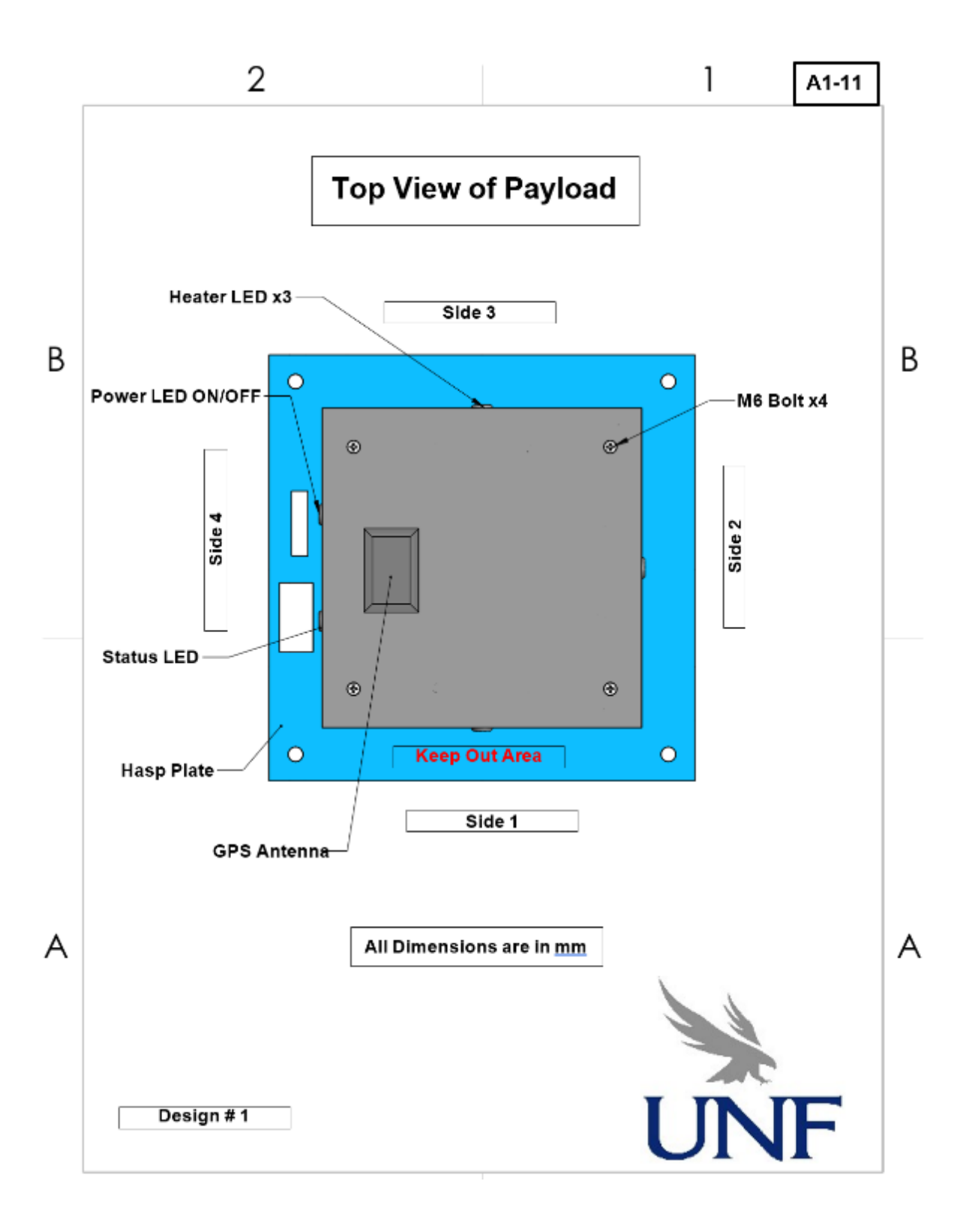


Fig. 15(j) Top view outside.

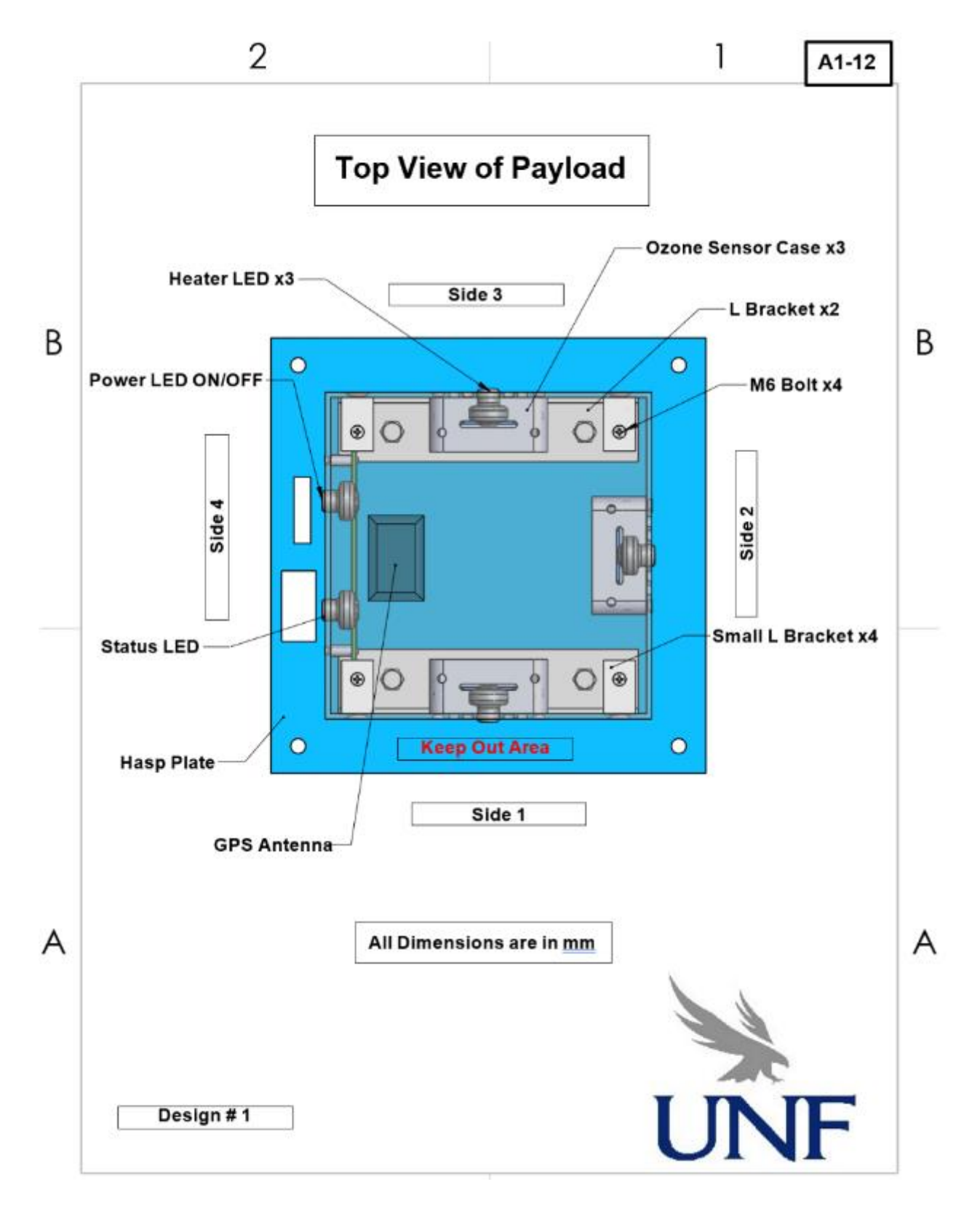


Fig. 15(k) Top view inside.

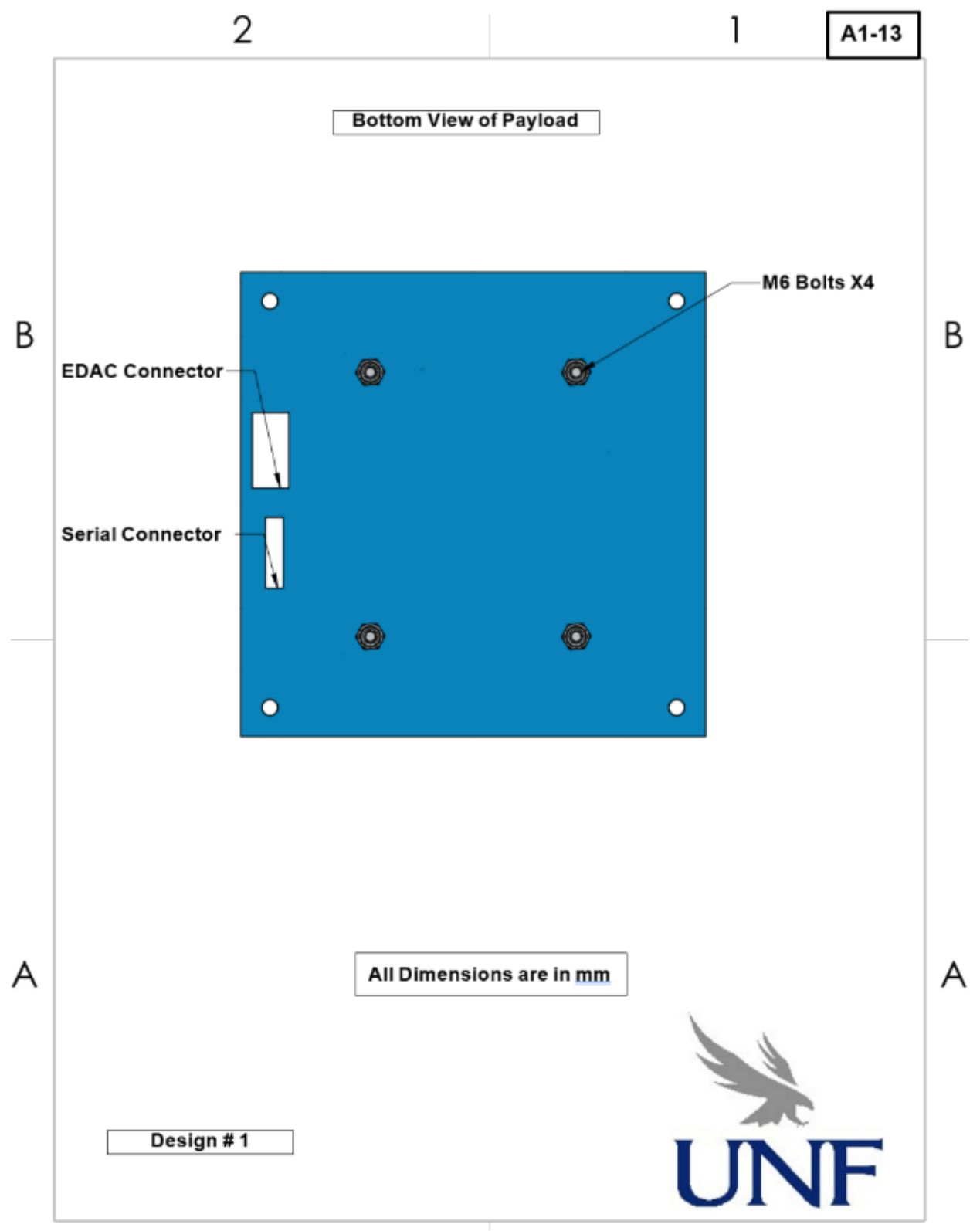


Fig. 15(l) Bottom view outside.

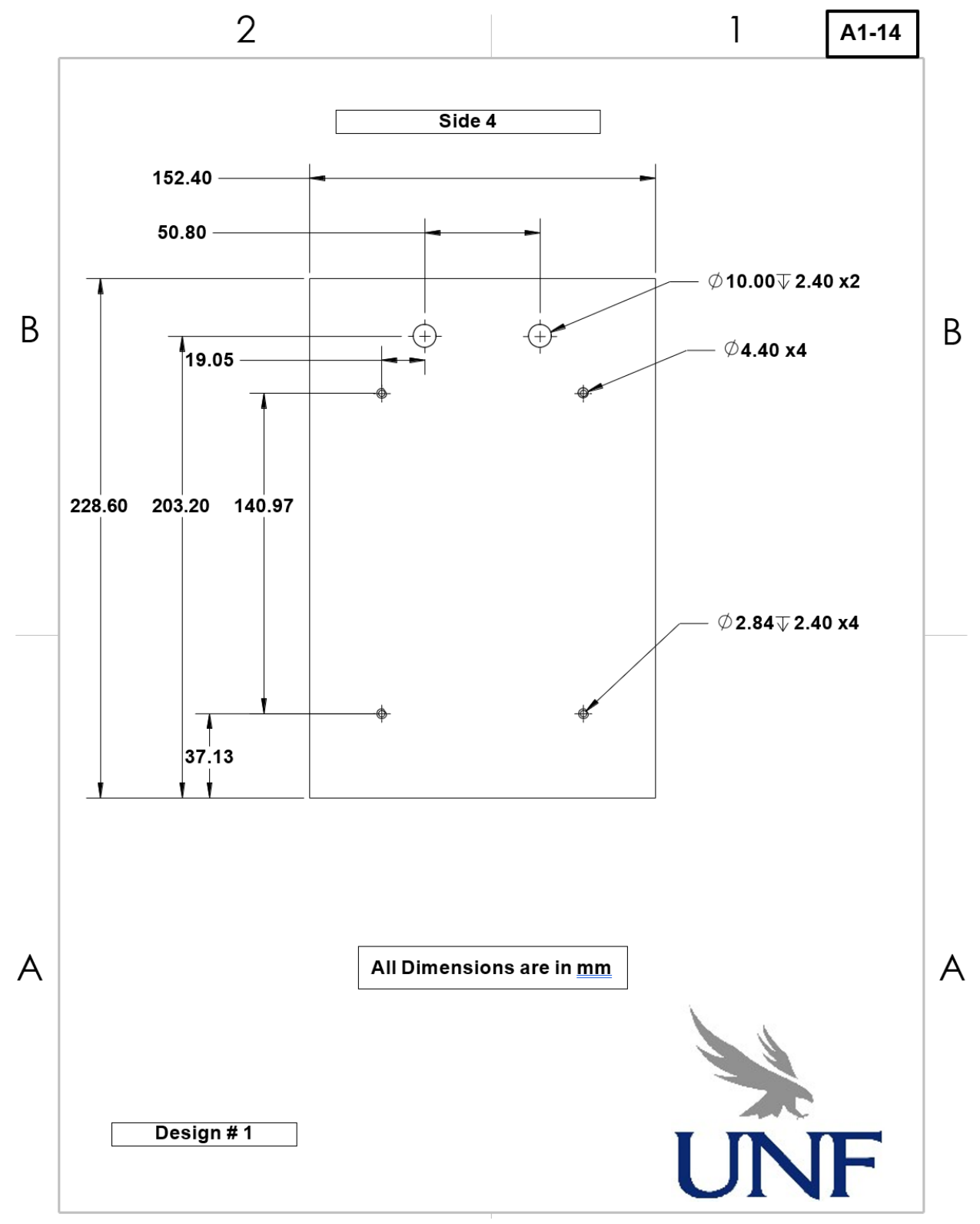


Fig. 15(m) Side 4 Holes.

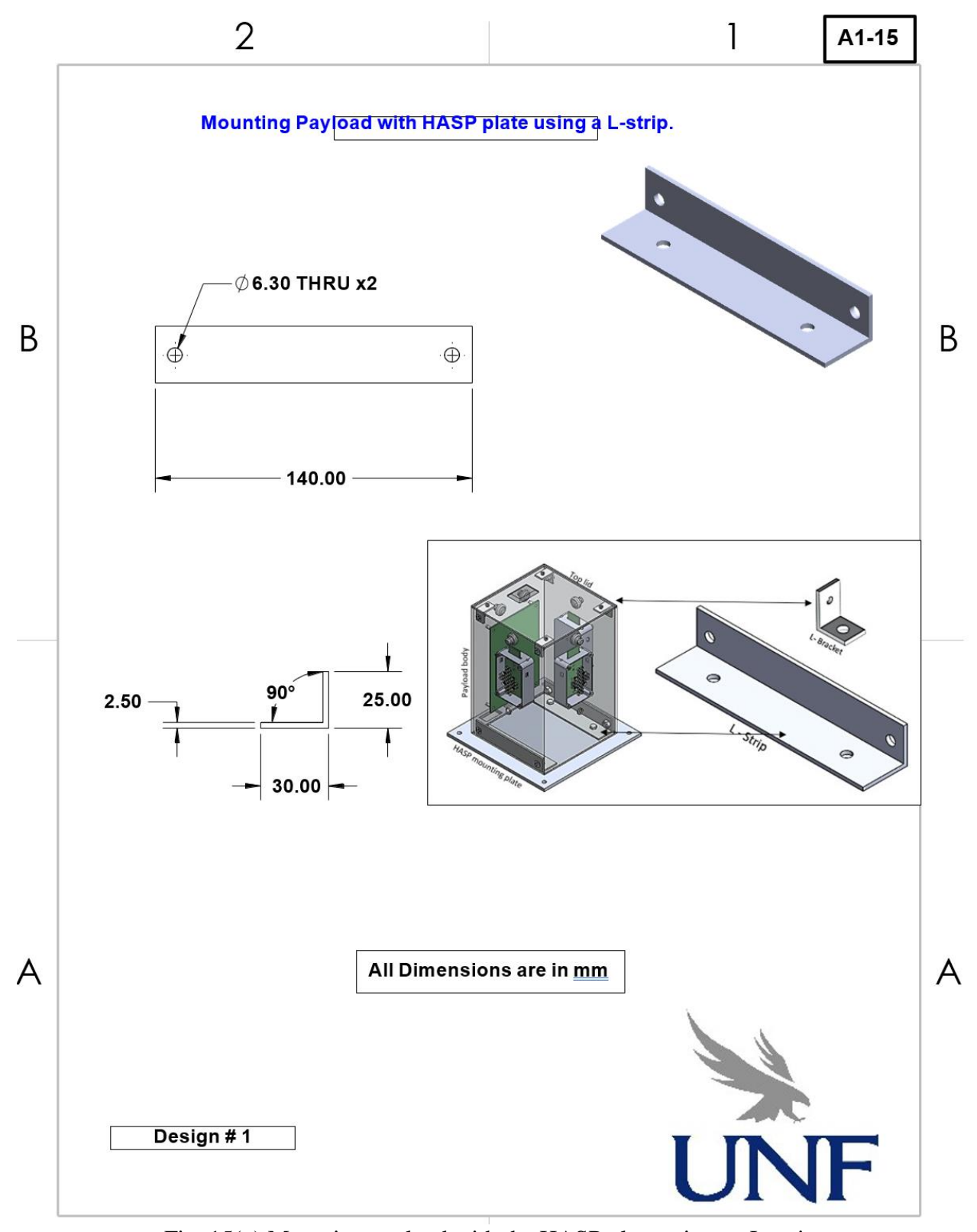


Fig. 15(n) Mounting payload with the HASP plate using an L-strip.

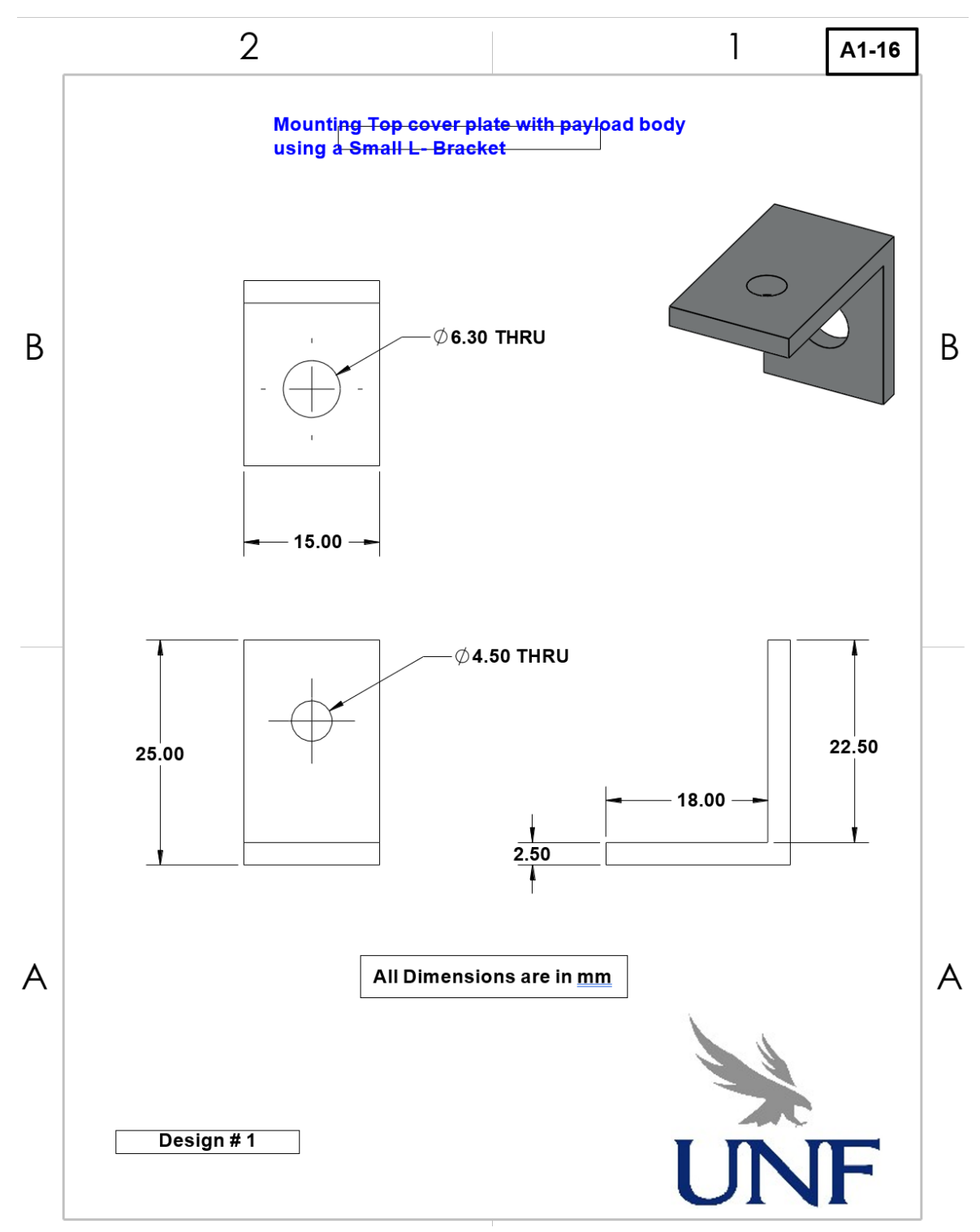


Fig. 15(o) Mounting payload with top plate using small L-bracket.

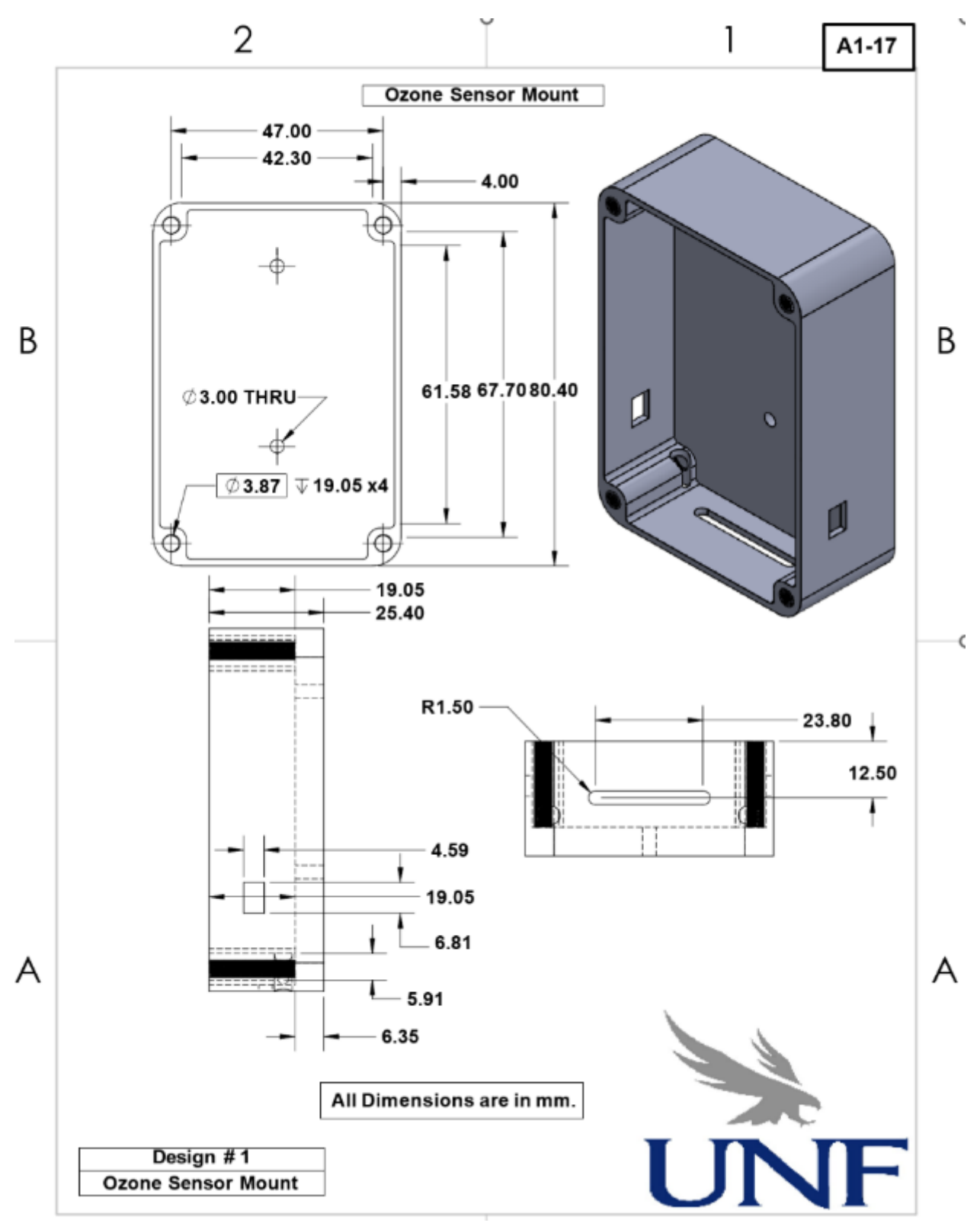


Fig. 15(p) Ozone sensor box mount.



Appendix -A (2)

Detailed Electronic Circuit Diagrams

Note: A separate file for detailed electronic circuits is provided with a proposal for a better font size and resolution.

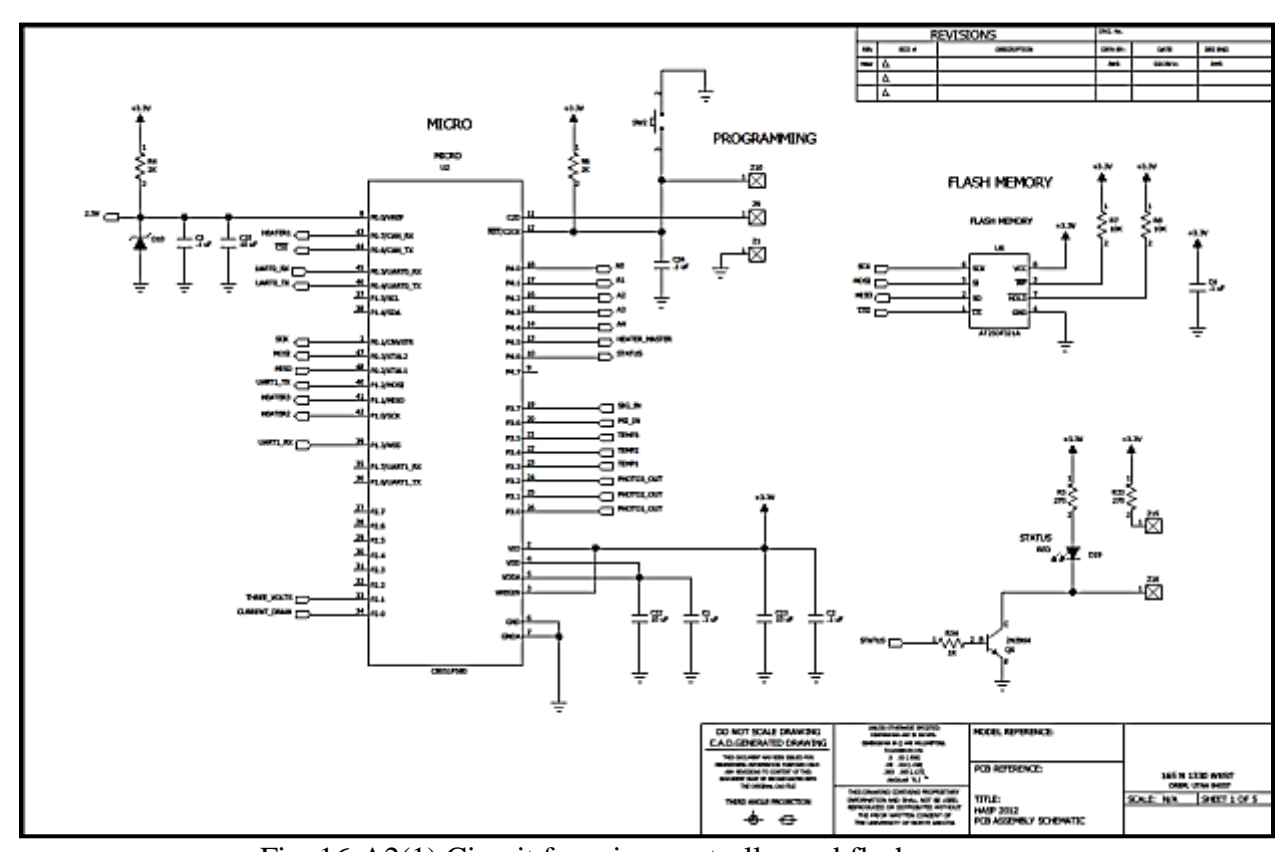


Fig. 16-A2(1) Circuit for microcontroller and flash memory

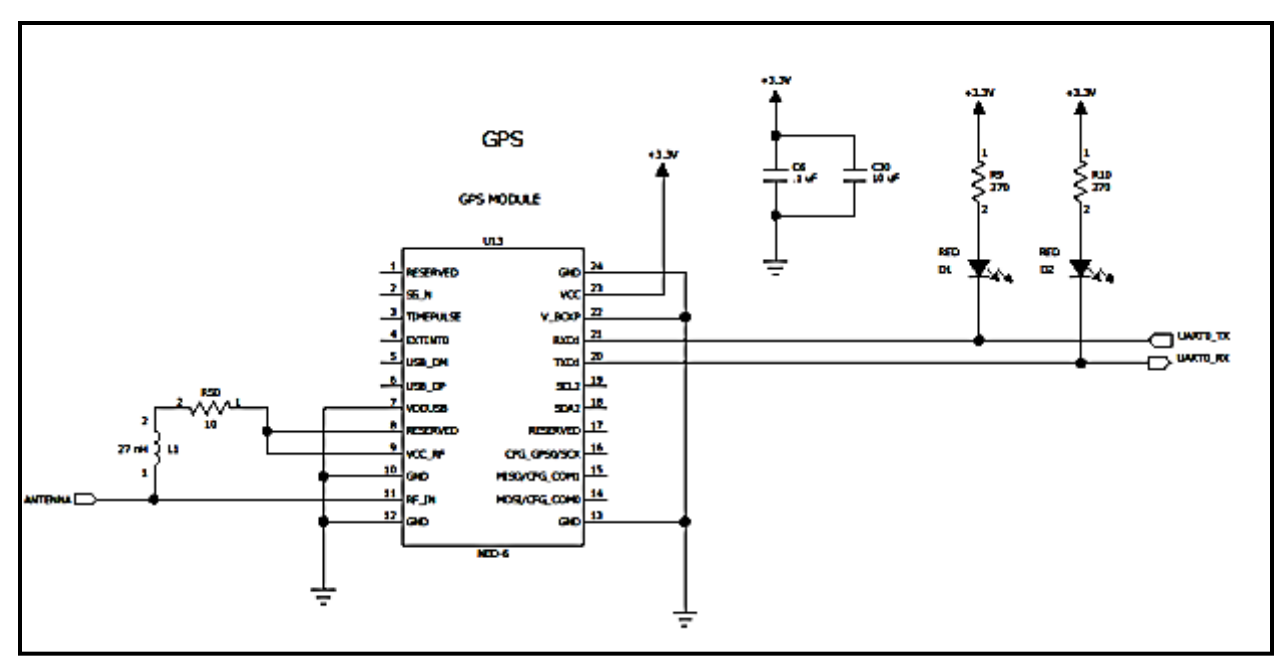


Fig. 16-A2(2) Circuit for GPS

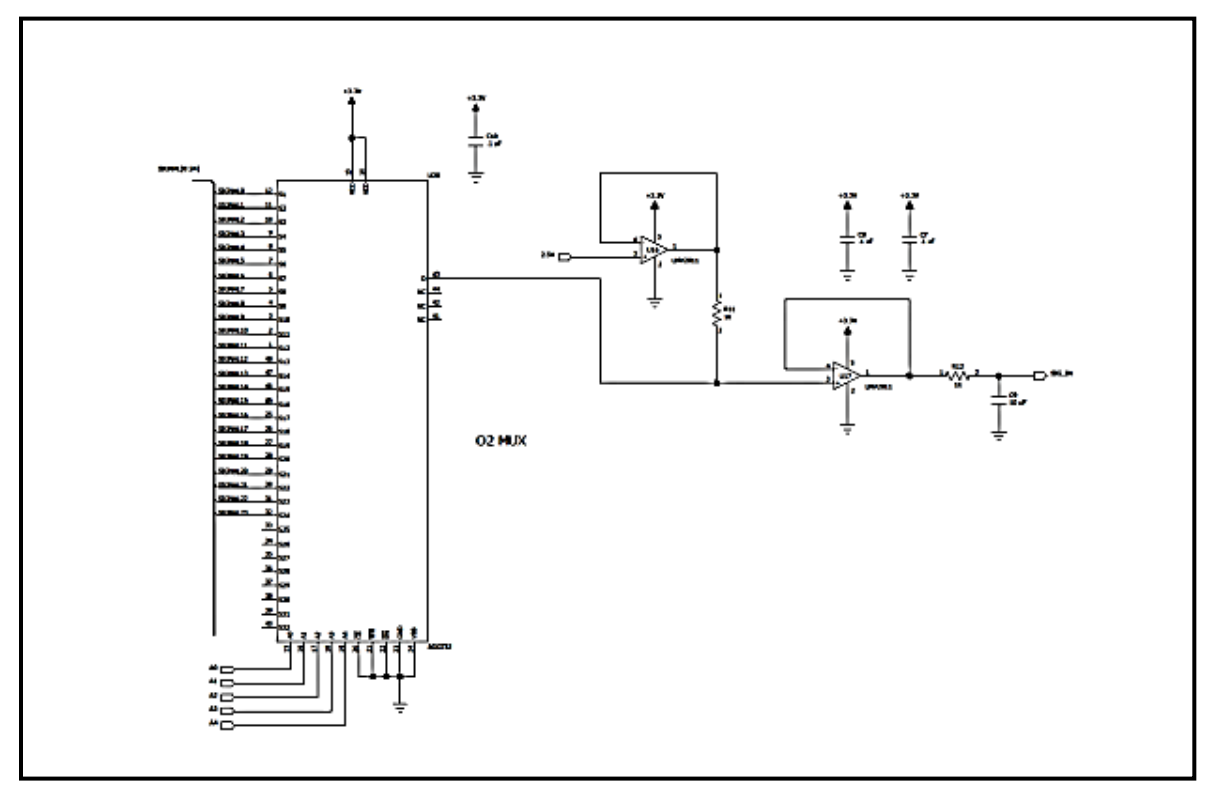


Fig. 16-A2 (3) Multiplexer circuit

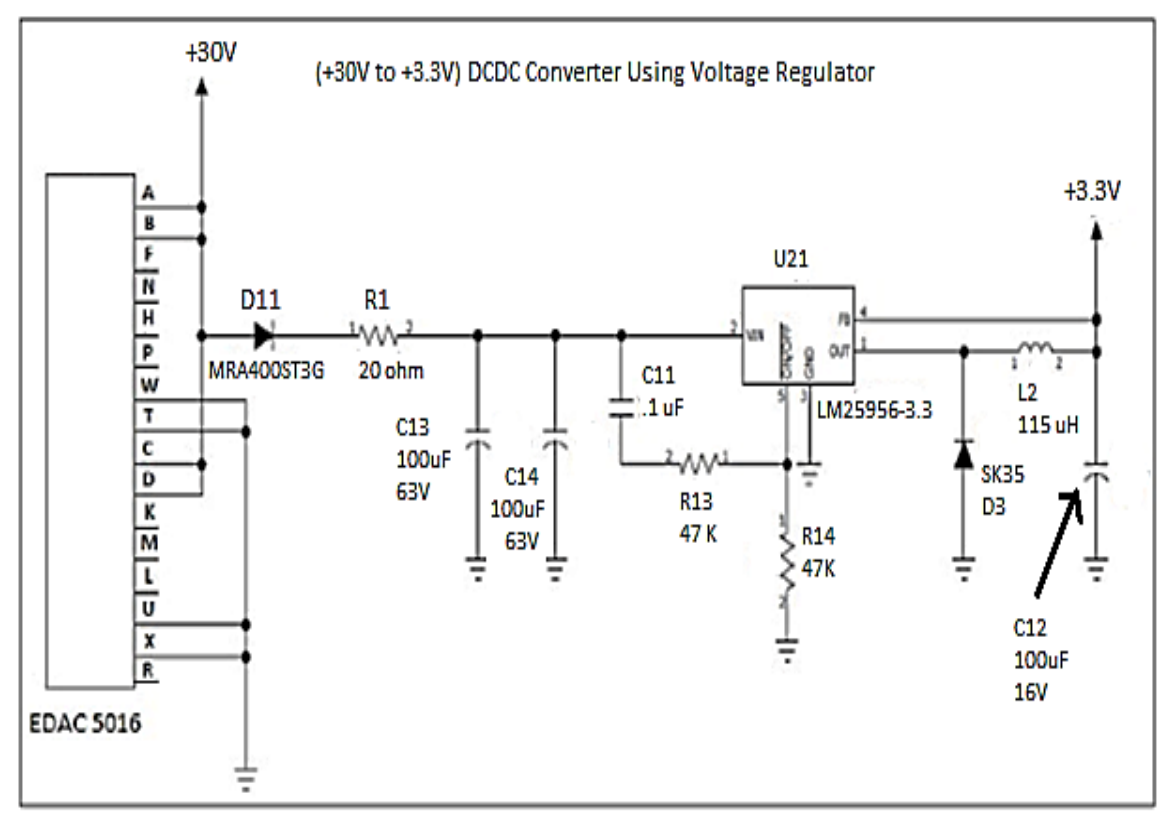


Fig. 16-A2 (4) Voltage regulation circuit

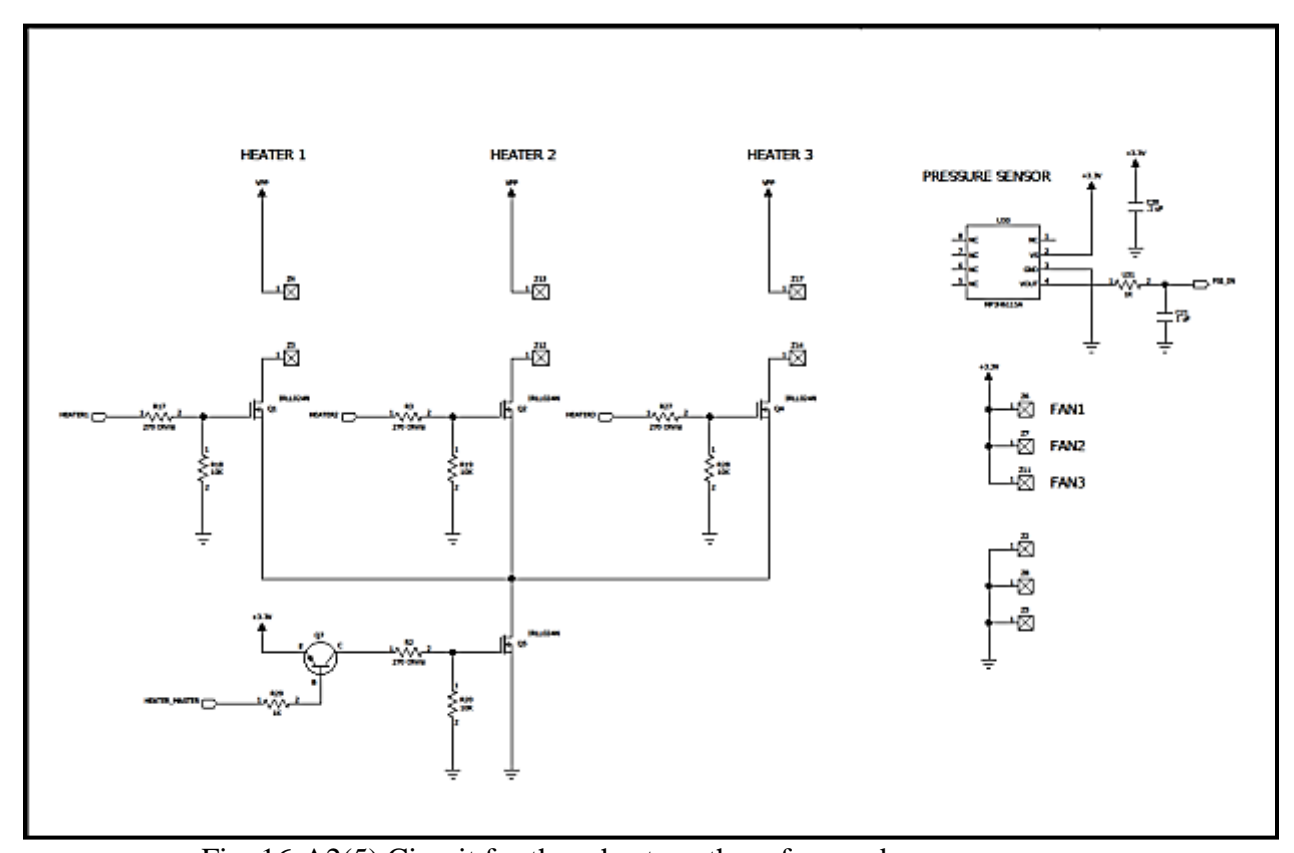


Fig. 16-A2(5) Circuit for three heaters, three fans and pressure sensor

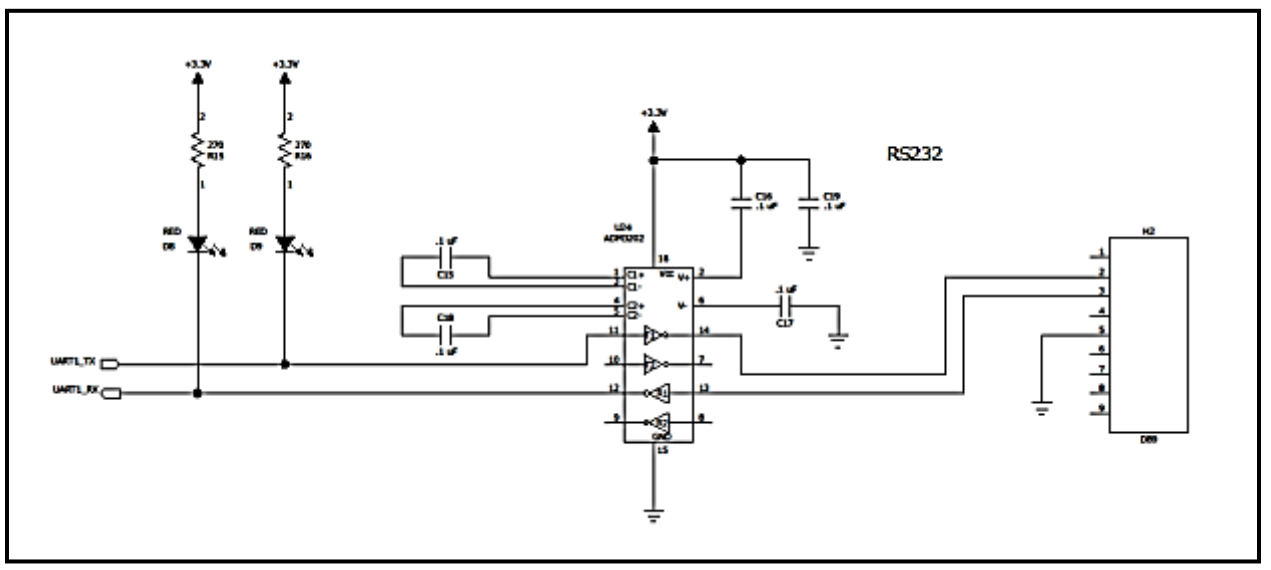


Fig. 16-A2(6) Circuit for RS232

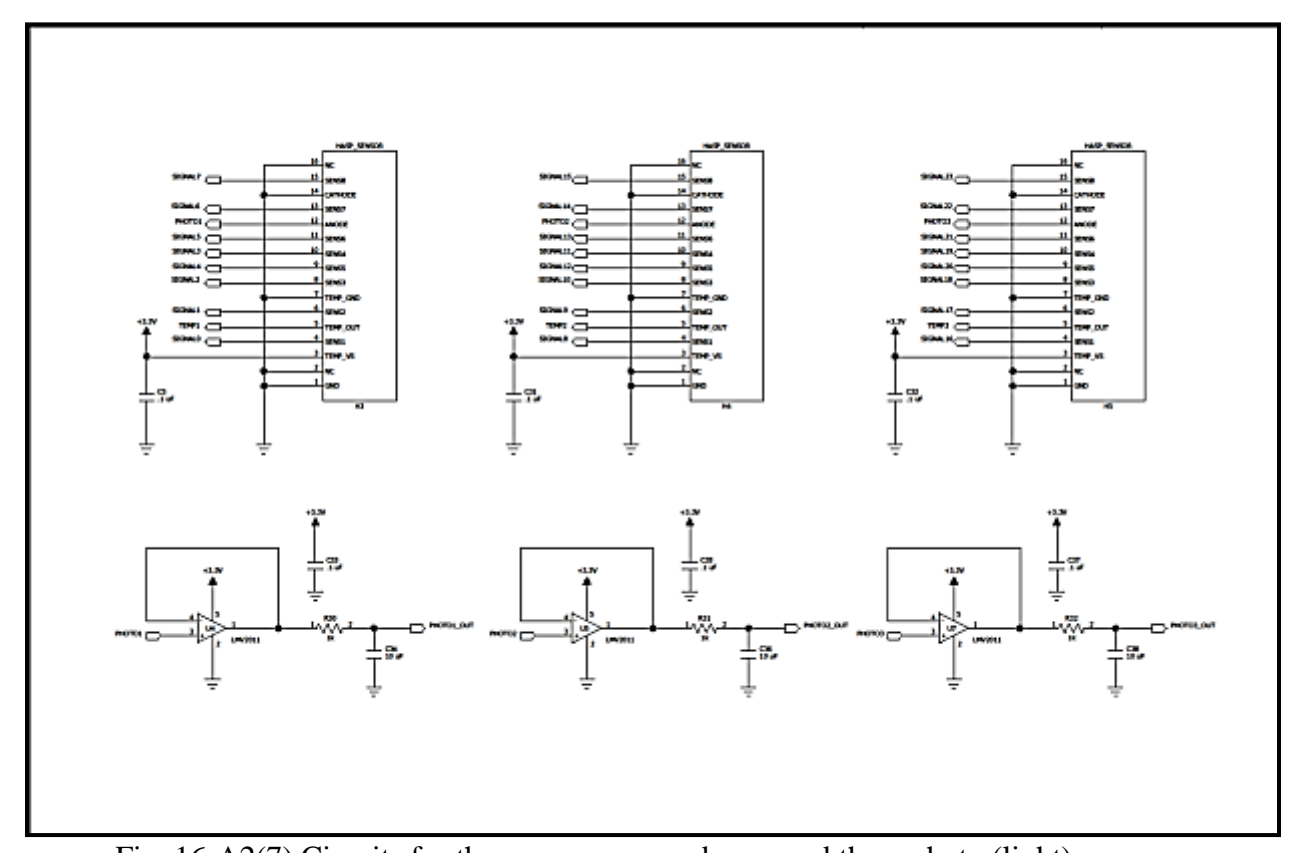


Fig. 16-A2(7) Circuits for three ozone sensor boxes and three photo (light) sensors.

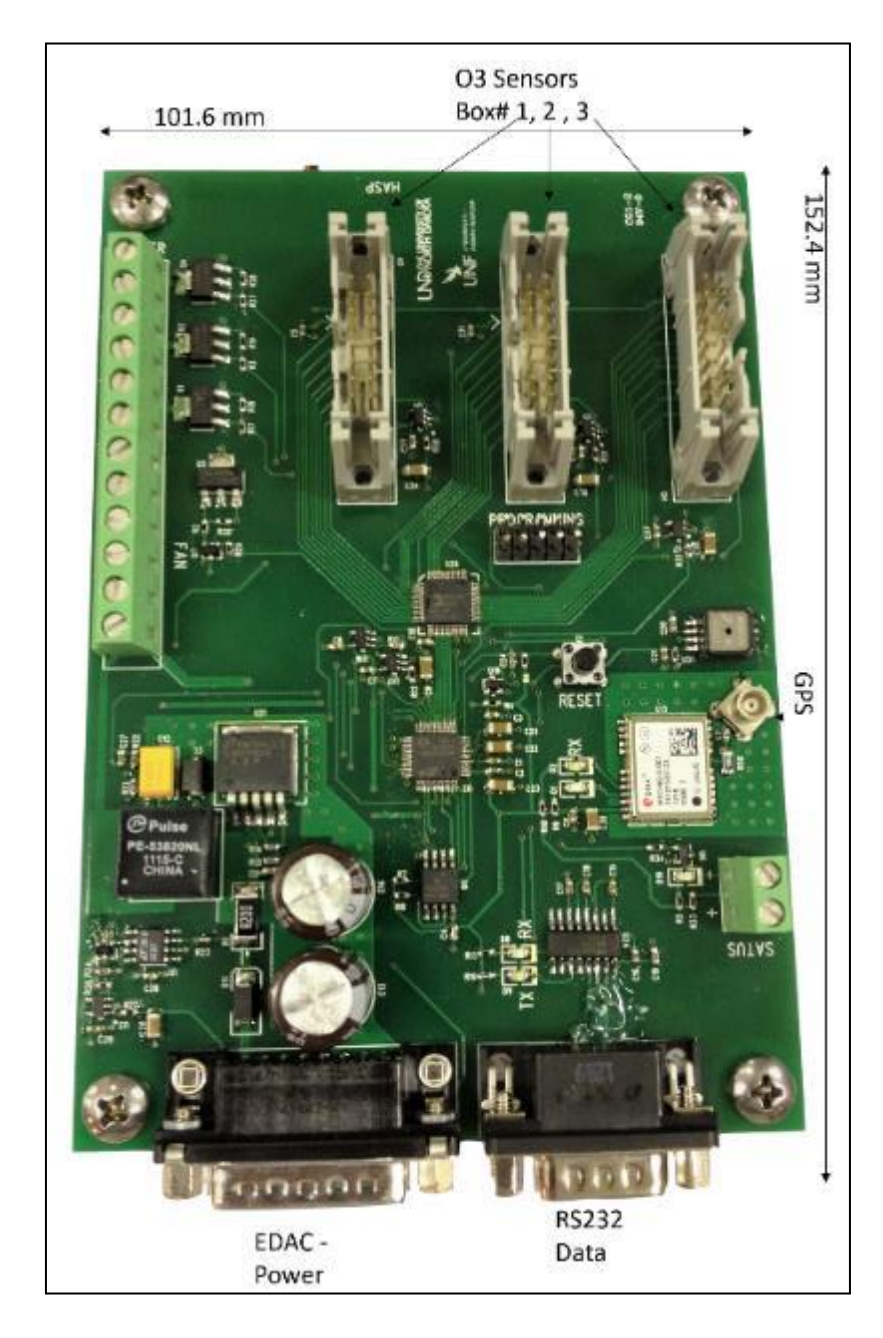


Fig. 16-A2(8) Photograph of microcontroller PCBs.

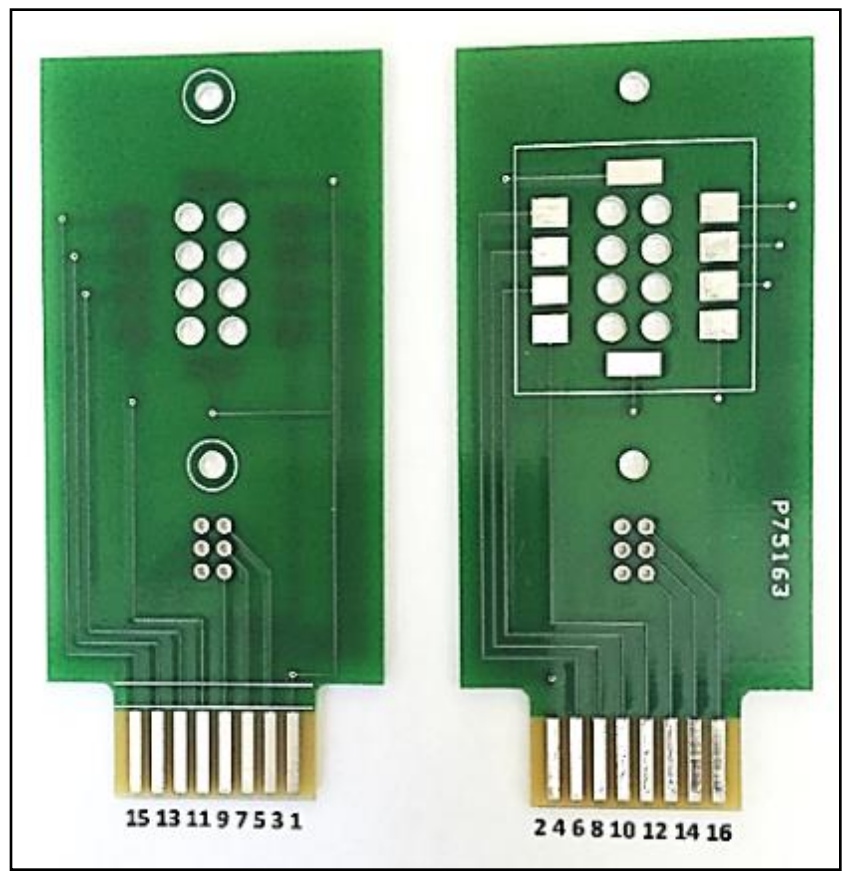


Fig.16-A2 (9) Pin number of sensor PCB.

Pin number per connector datasheet								
1	3	5	7	9	11	13	15	
Common	Temp Sensor	Temp Sensor	Temp Sensor	Gas Sensor	Gas Sensor	Gas Sensor	Gas Sensor	
Open	Gas Sensor	Gas Sensor	Gas Sensor	Gas Sensor	Light Sensor	Light Sensor	Pin not used	
2	4	6	8	10	12	14	16	
Pin number per connector datasheet								

Fig.16-A2(10) Pin information for connection of 16 pins female card edge connector with sensor PCB

Information of Components

MINCO Heater

http://www.minco.com/heater-configurator/model.aspx?PN=HK5573

Resistance of heater=30 ohms (4.8 Watts) Acrylic PSA operating voltage =3 to 9 volts Generate about 100 °C at about 8.00 to 9.00V

FAN

http://www.digikey.com/product-search/en?lang=en&site=us&KeyWords=259-1573-ND or equivalent.

MC25060V2-000U-A99

Digi-Key Part Number 259-1573-ND

Manufacturer Sunon Fans

Manufacturer Product Number MC25060V2-000U-A99

Supplier Sunon Fans

Description FAN AXIAL 25X6.9MM 5VDC WIRI

Detailed Description Fan Tubeaxial 5VDC Square - 25mm L x 25mm H Vapo-

Bearing™ 2.2 CFM (0.061m³/min) 2 Wire Leads

Card Edge Connector- Make: 3M or equivalent.

MCS16K-ND

16 pins female to connect Sensor PCB

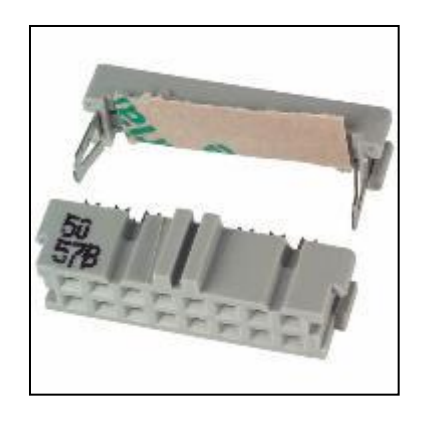
http://www.digikey.com/product-search/en?lang=en&site=us&KeyWords=MCS16K-ND



Socket connector Make:3M or equivalent.

16 pin female to connect microcontroller PCB

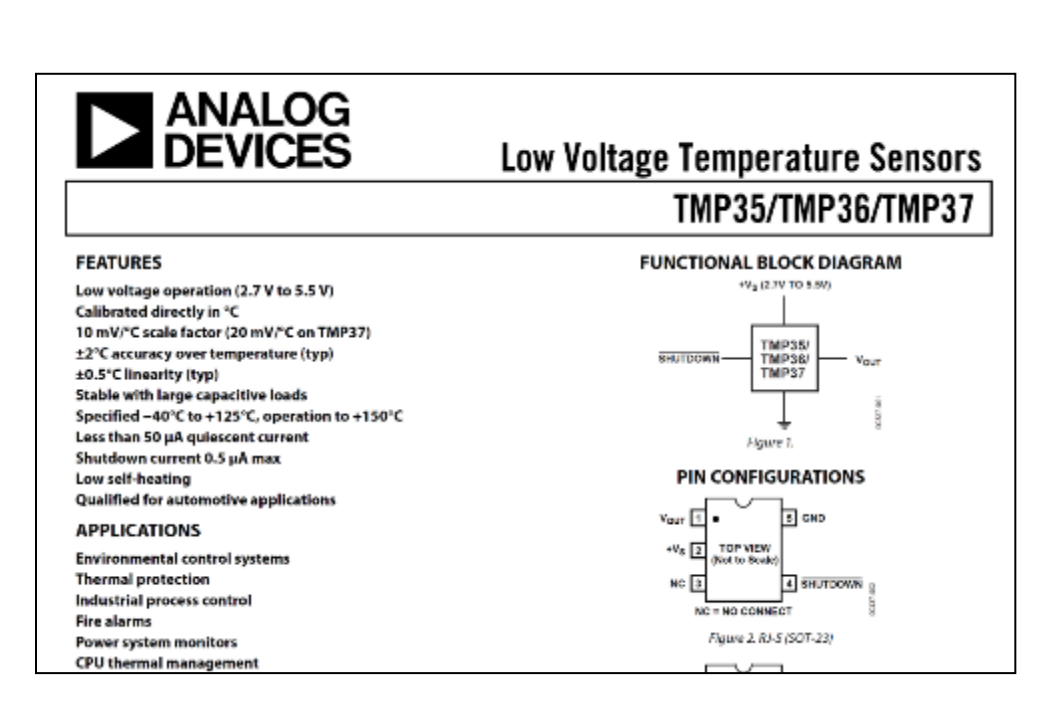
http://www.digikey.com/product-search/en?lang=en&site=us&KeyWords=3452-6600



Connector Make: 3M or equivalent.

16 male pin Header – to be mounted on microcontroller PCB http://www.digikey.com/product-detail/en/3408-6002/MHS16K-ND/138490





Appendix B NASA Hazard Tables

(a) Appendix B.1 Radio Frequency Transmitter Hazard Documentation

This is not applicable to the proposed payload.

HASP 2024 RF System Documentation				
Manufacture Model				
Part Number				
Ground or Flight Transmitter				
Type of Emission				
Transmit Frequency (MHz)				
Receive Frequency (MHz)				
Antenna Type				
Gain (dBi)				
Peak Radiated Power (Watts)				
Average Radiated Power (Watts)				

(b) Appendix B.2 High Voltage Hazard Documentation

This is not applicable to the proposed payload.

HASP 2024 High Voltage System Documentation				
Manufacture Model				
Part Number				
Location of Voltage Source				
Fully Enclosed (Yes/No)				
Is High Voltage source Potted?				
Output Voltage				
Power (W)				
Peak Current (A)				
Run Current (A)				

(c) Appendix B.3 Laser Hazard Documentation

This is not applicable to the proposed payload.

HAS	P 2024 Laser S	ystem Documentation		
Manufacture Model				
Part Number				
Serial Number				
GDFC ECN Number				
Laser Medium				
Type of Laser				
Laser Class				
NOHD (Nominal Ocular Hazard D	istance)			
Laser Wavelength				
Wave Type		(Continuous Wave, Single Pulsed, Multiple Pulsed)		
Interlocks		(None, Fallible, Fail-Safe)		
Beam Shape		(Circular, Elliptical, Rectangular)	
Beam Diameter (mm)		Beam Divergence (mrad)		
Diameter at Waist (mm)		Aperture to Waist Divergence (cm)		
Major Axis Dimension (mm)		Major Divergence (mrad)		
Minor Axis Dimension (mm)		Minor Divergence (mrad)		
Pulse Width (sec)		PRF (Hz)		
Energy (Joules)		Average Power (W)		
Gaussian Coupled (e-1, e-2)		(e-1, e-2)		
Single Mode Fiber Diameter				
Multi-Mode Fiber Numerical Ape	erture (NA)			
Flight Use or Ground Testing Use	?			

(d) Appendix B.4 Battery Hazard Documentation

This is not applicable to the proposed payload.

HASP 2024 Battery Hazard Documentation				
Battery Manufacturer				
Battery Type				
Chemical Makeup				
Battery modifications	(Must be NO)			
UL Certification for Li-Ion				
SDS from manufacturer				
Product information sheet from manufacturer				

(e) Appendix B.5 Pressurized system Hazard Documentation.

This is not applicable to the proposed payload.

HASP 2024 Pressurized System Hazard Documentation				
System Description				
Maximum Expected Operating Pressure (PSIG) or Vacuum				
Fluids (e.g. GN2, GHe, Air)*				
Notes				
SDS from manufacturer				

